LUT UNIVERSITY

LUT School of Energy Systems

LUT Mechanical Engineering

Miika Koskinen

MANUFACTURABILITY OF LAMINATED SQUIRREL CAGE ROTOR

Examiners: Professor Juha Varis

D. Sc. (Tech.) Mikael Ollikainen

TIIVISTELMÄ

Laminoidun häkkikäämityn induktioroottorin rakenne on yhdistelmä kompromisseja sähköisten ja mekaanisten ominaisuuksien väliltä. Mekaanisen lujuuden tulisi olla riittävä, kuitenkin uhraamatta liikaa hyötysuhteesta. Roottorin ominaisuuksia pystytään parantamaan suunnittelulla ja materiaalivalinnoilla. Muutokset rakenteessa tai materiaaleissa voi vaikuttaa vaihtoehtoihin valmistettavuuden suhteen, missä prosessien tai laitteiden kapasiteetti on rajallinen riippuen mittasuhteista tai materiaaliominaisuuksista. Tämä tutkimus keskittyy tarkastelemaan laminoidun häkkikäämityn roottorin vaihtoehtoja valmistettavuuden näkökulmasta.

Induktiokoneen rakenne käydään suppeasti läpi keskittyen laminoituun häkkikäämittyyn roottoriin. Tutkimuksessa käytettävän roottorin rakenne on yksi iteratiivisesta rinnakaissuunnittelusta syntynyt vaihtoehto ja valittu rakenne voi vielä muuttua. Roottorin rakenne on jaettu neljään pääosaan, lukuun ottamatta häkkikäämiä. Menetelmät tiedonhakuun ja tutkimuksen etenemiseen koostuvat kirjallisuuskatsauksesta, palavereista ja haastatteluista. Vaihtoehtoja rakenteeseen ja valmistettavuuteen tarkastellaan saatavilla olevan informaation puitteissa ja vaihtoehdoista kootaan ehdotettu konstruktio roottorille. Ehdotettu konstruktio koostuu roottorin pääosien suositelluista valmistusmenetelmistä sekä roottorin kokoonpanosta.

Tuntemattomien muuttujien määrä suunnittelussa, materiaaleissa ja prosesseissa tekee optimaalisten ratkaisujen löytämisestä hankalaa. Ehdotettu konstruktio on jossain määrin subjektiivinen yhdistelmä mahdollisista vaihtoehdoista valitulle rakenteelle tietyillä mitoilla ja materiaaleilla. Tuntemattomat muuttujat ja rajallinen määrä tietoa prosessien ja materiaalien suhteen rajoittaa tutkimuksen tarkkuutta. Valmistusmenetelmien ja materiaalien testauksilla ja lopullisen rakenteen suunnittelulla pystyisi parantamaan vaihtoehtoja valmistettavuuden suhteen.

ABSTRACT

Laminated squirrel cage induction rotor construction is combination of various compromises between mechanical and electrical properties. Mechanical strength of the rotor should be sufficient without sacrificing too much in terms of efficiency. Properties of the rotor can be improved via design and material choices. Any changes in either of them might affect the viable options regarding manufacturability of the rotor parts where capabilities of processes are limited depending on the dimensions or material properties. This thesis focuses on examining the options related to manufacturability of laminated squirrel cage rotor.

Induction machine construction is examined briefly focusing on the laminated squirrel cage rotor. Rotor construction used in this thesis is one option from iterative loop of concurrent engineering and design might be subject to change. Rotor construction is divided into four main parts, squirrel cage excluded, which are reviewed more closely. Methods for acquiring information and progressing forward include combination of literature review, meetings, and interviews. Options regarding design and manufacturability are reviewed based on the information available and proposed construction for the rotor is introduced. Proposed construction consists of recommended options for manufacturing the main rotor parts and assembly of the rotor.

Due to the number of unknown variables regarding design, materials, and processes, it's difficult to pinpoint optimal solutions for manufacturing of the main parts. Proposed construction is somewhat subjective combination of the reviewed options for the single design with specific dimensions and materials. Limitations of the research stem from unknown variables and lack of data. Manufacturability options for the rotor could be improved by further testing and finalizing the design in terms of dimensions and materials.

TABLE OF CONTENTS

LIST OF SYMBOLS AND ABBREVIATIONS

A Approach distance [mm]

d Depth of cut [mm]

D_d Drill diameter [mm]

D_m Mill cutter diameter [mm]

D_o Work diameter [mm]

f Feed [mm/rev]

f_r Feed rate [mm/min]

L Workpiece length [mm]

R_{MR} Material removal rate [mm^3/min]

T_m Machining time [min]

v Cutting speed [mm/min]

w Width of cut [mm]

θ Drill point angle [°]

APS   Atmospheric plasma spraying

CVD   Chemical vapor deposition

DFA   Design for assembly

DFM   Design for manufacturing

DFMA   Design for manufacturing and assembly

DGS   Detonation gun spraying

DLC   Diamond-like carbon

PTFE   Polytetrafluoroethylene

PVD   Physical vapor deposition

1   INTRODUCTION

Laminated squirrel cage induction machine rotor is reviewed in terms of manufacturability. This chapter covers background of the study, brief introduction for the working principle and configuration of induction machine and some viable manufacturing methods for the rotor parts are reviewed.

1.1   Background of the study

This thesis is part of a collaboration project regarding design of 2 MW 15 000 rpm active magnetic bearing induction machine. The project is divided into different areas that progress forward by iterative loop of concurrent engineering. This thesis focuses on the manufacturability options regarding the laminated squirrel cage rotor. Framework in terms of baseline materials and rotor design is given and purpose of this thesis is to review options regarding manufacturability and assembly of the rotor parts. Baseline dimensions and materials for the rotor include length of the shaft being 1500 mm made from S355 and length of the lamination stack being 400 mm made from S960. Lamination disk dimensions include thickness of 5 mm and diameter of 254 mm. Materials and dimensions might be subject to change as project progresses, but manufacturability aspects are reviewed mainly for these parameters.

1.2   Induction machine

Induction machine is commonly used as electrical drive and generator due to simple construction and relatively high efficiency. Induction motor essentially consists of wound stator and either wound rotor or squirrel cage rotor depending on the construction. (Melkebeek 2018, p. 117.) Squirrel cage and slip-ring induction machines use three-phase current, which connected to three-phase stator winding, generates rotating current layer and rotating field. Angular velocity of the rotation depends on the frequency and number of poles. Rotating field causes electromotive force in the rotor, which combined with short-circuited windings produces current in the rotor. Current in the rotor produces torque that tries to synchronize the rotor with the rotating field. Ratio of frequency between synchronous rotation of the field and the rotor is called slip. Magnetomotive forces of the rotor and stator, generated by the current, affect the magnetic field of the machine. When induction machine

is used as generator, rotor spins faster than synchronous speed with negative slip and induces electromotive force which produces current and torque in the rotor. Torque from the rotor opposes the mechanical rotation and generates current in the stator. (Melkebeek 2018, pp. 127-129.)

Efficiency of the induction machine depends on combination of loss components. Loss components can be divided into constant and variable losses. Copper losses in the induction machine as well as additional load losses are variable losses which are relative to the load. Iron losses and mechanical losses are constant in relation to load. (Aarniovuori et al. 2018, p. 1253.) For laminated squirrel cage induction machine there are number of ways to reduce loss components. Copper losses in the stator can be reduced by increasing the amount of copper, decreasing number of windings, and using longer stator core. Copper losses in the rotor can be reduced by modifying the cross-section and material of the squirrel cage. Iron losses can be reduced by longer rotor core with thinner laminations made from electrical steel with better electromagnetic properties. Windage and friction losses can be reduced by eliminating rotor fan and improving bearings. Additional load losses can be reduced by optimization of air gap and rotor centricity as well as modifying stator slots. (Agamloh & Kaufman Dyess 2007, p. 66.)

1.3   Rotor design

Rotor design is balanced between mechanical and electromagnetic properties. Mechanical strength of the rotor should be sufficient to withstand high stresses caused by high peripheral speeds. Friction losses vary between designs and rotors with obstructions, like slits or bars on the surface tend to have higher friction losses compared to smooth surface rotors. Electromagnetic properties vary between the rotor designs. Slip of the rotor reflects the efficiency of the motor and it should be as low as possible. To further improve electromagnetic properties, magnetic field should have deeper penetration into the rotor while power factor should be kept high. Poor electromagnetic properties of solid slitted rotor can be improved by implementing a squirrel cage design into the rotor. Efficiency can be further improved with laminated rotor where air gap doesn't have to be as large as in solid rotor due to great electromagnetic properties. (Durantay et al. 2013, pp. 2-4.)

1.3.1 Solid rotor

Solid rotor topologies include smooth, slitted, coated, and caged rotors. Smooth solid rotor is the most basic to design and manufacture, but the efficiency of smooth rotor is lowest due to high eddy current losses and lack of path for magnetic flux. Slitted solid rotor design improves the flux permeability while reducing eddy currents. Drawbacks of the slitted rotor include weaker structure and gas friction loss at high speeds which may offset the benefits gained from reduced eddy currents. Solid rotor with copper coating improves the efficiency compared to solid smooth rotor with a drawback of poor power factor due to distance between irons of stator and rotor. Caged solid rotor has higher efficiency and power density compared to coated rotor due to combined benefits of squirrel cage and solid rotor. Due to difficulties in manufacturing, caged solid rotor has open slots on the surface instead of holes for the cage which limits the mechanical strength of the structure. Laminated rotor with squirrel cage has higher efficiency compared to the solid rotor designs with the drawback of weaker structure and challenges in manufacturing. (Boglietti et al. 2014, pp. 2952-2953.)

Amount of rotor components vary depending on the construction. Smooth solid rotor is bare-bones structure which can be improved by adding high conductivity material to the outer surface of the rotor. High conductivity materials tend to be quite soft so there may be requirements for some support material or structure for those. Losses can be further decreased by laminated rotor stack instead of solid rotor. Lamination stack, depending on the disk thickness, may require some support as well.

1.3.2 Laminated rotor

Eddy currents generated in the rotor and related losses can be decreased by using thinner insulated laminations where eddy currents are restrained within single lamination instead of wandering around the rotor increasing losses (Manney 2017). According to Barta, rotor lamination material should have decent electromagnetic properties as well as mechanical strength to withstand stresses. Favorable properties combined with decent mechanical strength can be found in electrical steels. Depending on the operating speeds, solid rotor might be better option due to higher bending stiffness and critical speed which limits laminated rotor. (Barta et al. 2019, p. 6770.) Properties of electrical steels can be seen in Figure 1 below.
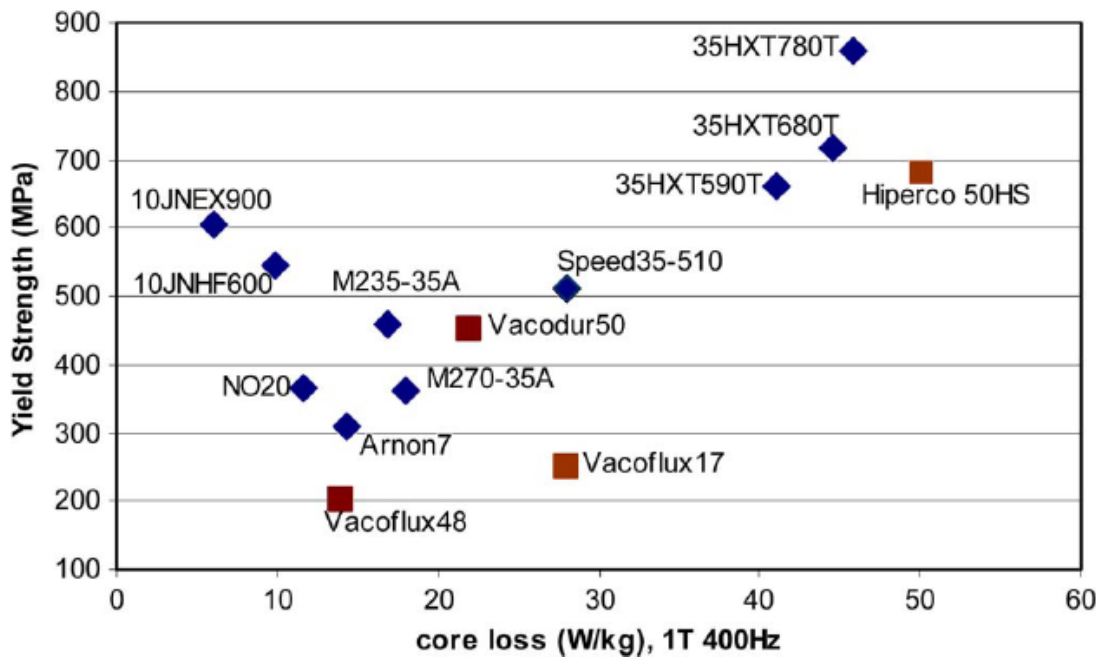
Figure 1. Properties of electrical steels (Boglietti et al. 2014, p. 2950).

1.4   Squirrel cage

Squirrel cage is short-circuited cage that is affected by the rotating electromagnetic field which induces voltage in the squirrel cage bars creating rotational movement of the rotor. Squirrel cage induction machines are asynchronous where rotation of the rotor is delayed from the electromagnetic field by the amount of slip. (Cavallo n.d.) According to Barta squirrel cage material properties should have high conductivity and high mechanical strength in order to endure the stress in high speed. Due to high temperatures, pure copper would not be durable enough and alternative cage material could be found in copper alloys which offer higher mechanical strength in a tradeoff for lower conductivity. (Barta et al. 2019, p. 6770.) Copper alloy properties for squirrel cage can be seen in Figure 2 below.
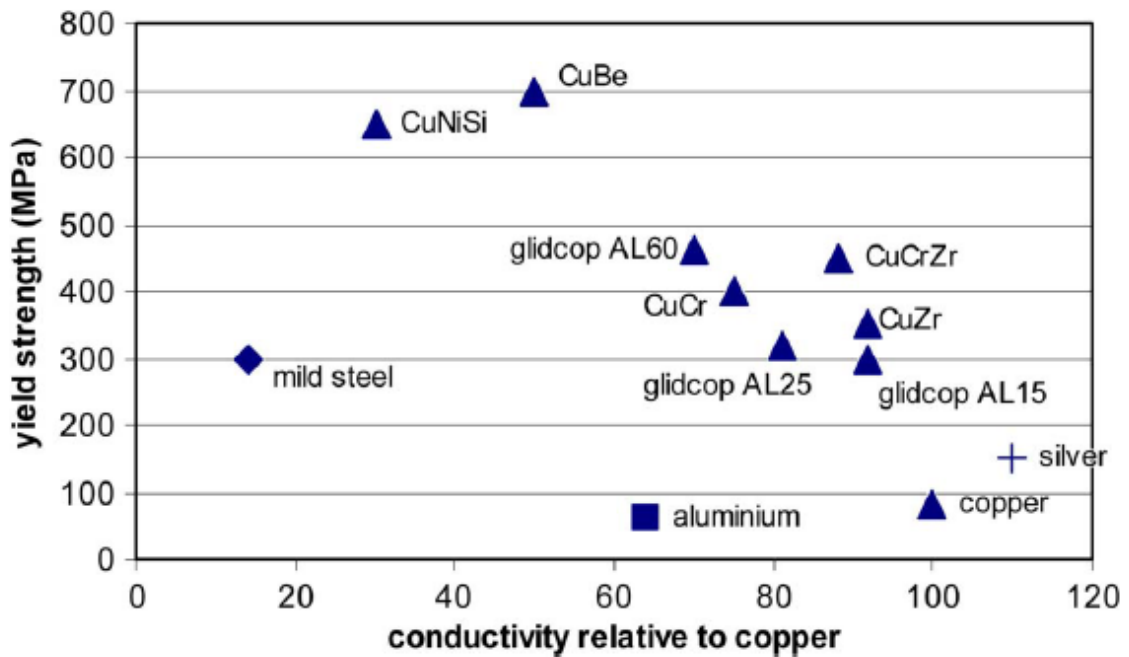
Figure 2. Copper alloy properties for squirrel cage (Boglietti et al. 2014, p. 2951).

1.5   Materials and manufacturing methods for squirrel cage rotor parts

Baseline material options considered for the rotor include S355 for the shaft and end disk nuts. Strenx 960 (SSAB) for disks, Inconel alloy (Special Metals Corporation) for end disks and copper zirconium alloy for squirrel cage. S355 is widely used cost-effective structural steel with yield strength of 355 MPa and tensile strength between 470-630 MPa (Velling 2019). According to SSAB website, Strenx 960MC is hot rolled high-strength structural steel with yield strength of 960 MPa and tensile strength between 980-1250 MPa. Available thickness being 3-10 mm. (SSAB n.d.a.) According to Special Metals product handbook, Inconel alloys are corrosion resistant nickel alloys that retain their mechanical properties at high temperatures. There are different properties between Inconel grades based on chemical composition. (Special Metals n.d. pp. 8-16.) Copper zirconium alloy contains 0.05-0.15% zirconium which improves the mechanical properties while retaining high conductivity (Copper Development Association n.d.). Essential manufacturing methods for the rotor would be turning, milling, boring, cutting and forging.

1.5.1 Machining processes

Machining processes can be divided into generating and forming processes depending on the machining methods. Generating processes include basic turning and milling processes

where feed trajectory of the cutting tool determines the shape of machined piece. Forming processes include drilling and broaching where machined shape is equal to the tool shape. Generating and forming processes can be combined where turning or milling process machines the cut in the shape of the tool. Machined workpieces can be divided into rotational and nonrotational depending on the geometry. Relative motion between workpiece and cutting tool varies between machining processes. Rotational workpiece processes such as turning and boring rotate the workpiece, drilling rotates the tool and nonrotational workpiece processes such as milling or sawing use linear motion in workpiece and either linear motion or rotational motion in the cutting tool. (Groover 2010, pp. 507-510.) Typical tolerances and surface roughnesses of traditional machining processes can be seen in Figure 3 below.

Machining Operation	Tolerance		SR (AA)		Machining Operation	Tolerance		SR (AA)	
	mm	(in)	μm	(μ-in)		mm	(in)	μm	(μ-in)
Turning, boring			0.8	(32)	*Reaming*			0.4	(16)
Diameter $D < 25$ mm	±0.025	(±0.001)			Diameter $D < 12$ mm	±0.025	(±0.001)		
25 mm $< D < 50$ mm	±0.05	(±0.002)			12 mm $< D < 25$ mm	±0.05	(±0.002)		
Diameter $D > 50$ mm	±0.075	(±0.003)			Diameter $D > 25$ mm	±0.075	(±0.003)		
Drilling[a]			0.8	(32)	*Milling*			0.8	(32)
Diameter $D < 2.5$ mm	±0.05	(±0.002)			Peripheral	±0.025	(±0.001)		
2.5 mm $< D < 6$ mm	±0.075	(±0.003)			Face	±0.025	(±0.001)		
6 mm $< D < 12$ mm	±0.10	(±0.004)			End	±0.05	(±0.002)		
12 mm $< D < 25$ mm	±0.125	(±0.005)			*Shaping, slotting*	±0.025	(±0.001)	1.6	(63)
Diameter $D > 25$ mm	±0.20	(±0.008)			*Planing*	±0.075	(±0.003)	1.6	(63)
Broaching	±0.025	(±0.001)	0.2	(8)	*Sawing*	±0.50	(±0.02)	6.0	(250)

Figure 3. Typical tolerances and surface roughnesses of traditional machining processes (Groover 2019, p. 533).

Turning process rotates the work piece and removes material with cutting tool moving in linear motion along the machined piece. Turning process can be divided into roughing cut and finishing cut. Roughing cut uses parameters resulting in high removal rate and rough surface quality. Finishing cut dials back the parameters used in the roughing cut in order to achieve better surface finish. Power requirement for the turning process can be calculated from cutting force, radius of the work piece and rotational speed. Cutting force is tangential force towards the cutting tool, other forces in the turning process are feed force and radial force. Feed force is longitudinal force parallel to the work piece towards the cutting tool. Radial force, perpendicular to the other forces and the work piece surface, comes from the workpiece towards the cutting tool. Feed force and radial force are difficult to measure but can be experimentally figured out while cutting force can be measured during turning.

(Davim et al. 2019, pp. 93-94.) Machining time T_m and material removal rate R_{MR} for turning process can be calculated with equations below (Groover 2019, p. 467):

$$T_m = \frac{\pi D_o L}{fv} \tag{1}$$

$$R_{MR} = vfd \tag{2}$$

In equation 1 for machining time T_m, D_o is work diameter, L is workpiece length, f is feed, and v is cutting speed. In equation 2 for material removal rate R_{MR}, v is cutting speed, f is feed, and d is depth of cut. (Groover 2019, p. 467.)

Drilling process creates circular holes into the work piece with relative rotation between drill bit and the work piece. Common twist drill removes the metal swarf from the hole via helical flute. Quality of the drilled hole can be improved with reaming, honing processes and in the case of through hole there might be rough edge in need of deburring. Hole diameter might vary slightly depending on the thermal expansion rate of the workpiece material. (Davim et al. 2019, p. 96.) Machining time T_m for the drilling process can be calculated with equation below (Groover 2019, p.476):

$$T_m = \frac{d + A}{f_r} \tag{3}$$

In equation 3 for machining time T_m for drilling process, d is hole depth which is same as thickness in the case of through hole, A is approach distance which takes the conical cutting edge into account when calculating drilling time, f_r is feed rate. Approach distance A can be calculated with equation below (Groover 2019, p. 476):

$$A = 0.5D_d \tan\left(90 - \frac{\theta}{2}\right) \tag{4}$$

In equation 4 for approach distance A, D_d is drill diameter and θ is drill point angle. Material removal rate R_{MR} in drilling process without taking approach distance into account can be calculated with equation below (Groover 2019, p. 476.):

$$R_{MR} = \frac{\pi D_d^2 f_r}{4} \qquad (5)$$

In equation 5 for material removal rate, D_d is drill diameter and f_r is feed rate. There are multiple processes related to drilling which improve the quality or add some features to the drilled hole such as reaming and tapping. (Groover 2019, pp. 476-477.)

Boring process enlarges pre-existing holes from drilling and casting operations by using single point cutter on a tungsten carbide boring bar. Boring is similar process to turning but instead of removing material on the outer surface boring hollows out the workpiece on the inner surface. Boring can be done on a lathe and for larger workpieces boring can be done with boring mill. (Davim et al. 2019, pp. 95-96.)

Lathes come in various degrees of automation, which affects the parameters regarding costs, production, and features. Tradeoff for high production rate and relatively low labor costs of automatic machining is higher equipment and tooling costs and limited flexibility in terms of changes compared to manual machining. There are parameters regarding cutting tool, lubricant and machining itself which should be selected appropriately. Machinability index of the material indicates the degree of difficulty in terms of machining compared to mild steel, which affects the quality of the finished surface as well as required properties and wear and tear of the machine. Turning and boring tolerances depend on machinability of the material but can be improved by using diamond-tipped tools. (Booker & Swift 2013, pp. 176-178.) Figures 4 & 5 below show 4-axis CNC lathe with 12-station turret, capable of turning, milling, and drilling operations.
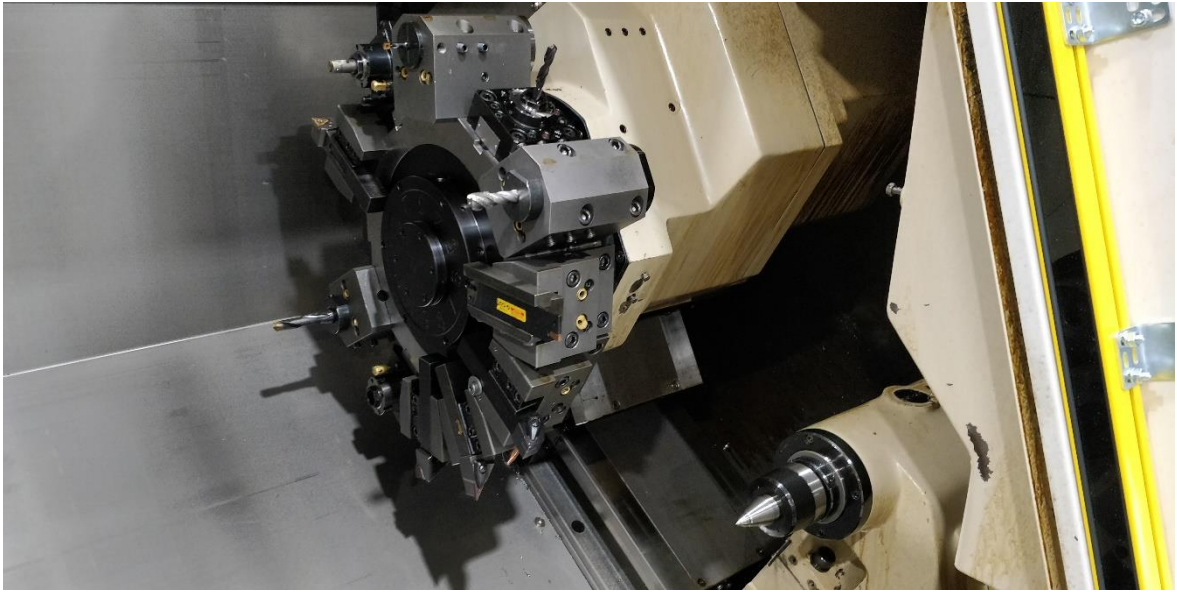
Figure 4. 4-axis CNC lathe turret and tailstock.

Figure 5. 4-axis CNC lathe 3-jaw chuck.

Milling process uses rotating circular multi-point cutter to cut out material from the machined part. Depending on the rotation direction of the cutting tool and feed direction, milling process is either up milling or down milling. In up milling, rotation of the cutter is opposite to the feed direction of the work piece whereas in down milling rotation of the cutter is in the same direction as the feed of the workpiece. Up milling tends to be better option between the two since it produces better surface finish, better tool life and isn't as selective in terms of surface properties of the machined piece. Milling processes can be divided into

peripheral, face and end milling. Both peripheral milling and face milling processes rotate circular cutting tool on an axis related to workpiece surface, one on parallel axis and one on perpendicular axis. Both peripheral and face milling circular cutting tools have multiple cutting points each of which function as single point cutting tool. End milling process rotates cylindrical cutting tool mainly perpendicular to the work piece with an option of variable angle. Long and narrow cutting tool with teeth or inserts at the surface is capable of machining shapes such as curves and pockets. (Davim et al. 2019, pp. 94-95) Machining time T_m in milling process can be calculated with equation below (Groover 2019, p. 483):

$$T_m = \frac{L+A}{f_r} \tag{6}$$

In equation 6 for machining time T_m for milling process, L is workpiece length, A is approach distance and f_r is feed rate. Approach distance varies depending on the milling process and position of the cut. Approach distance A for slab milling, centered face milling and offset face milling respectively can be seen in equations below (Groover 2019, pp. 483-484)

$$A = \sqrt{d(D_m - d)} \tag{7}$$

$$A = 0.5(D_m - \sqrt{D_m{}^2 - w^2}) \tag{8}$$

$$A = \sqrt{w(D_m - w)} \tag{9}$$

In Equations 7,8, and 9 for approach distance A in slab, centered face and offset face milling respectively, d is depth of cut, D_m is mill cutter diameter, and w is width of cut. In the case of centered face milling, if workpiece width is equal or greater than cutter diameter, approach distance is half of the cutter diameter. Material removal rate R_{MR} can be calculated with equation below (Groover 2019, pp. 482-484):

$$R_{MR} = wdf_r \tag{10}$$

In equation 10 for material removal rate R_{MR} in milling process, w is width of cut, d is depth of cut and f_r is feed rate. This equation doesn't take approach distance into account and is valid when approach distance shrinks to zero and there is full contact between the cutter and the workpiece. (Groover 2019, pp. 482-483.)

Milling process variations include horizontal and vertical milling as well as CNC machines. Each variation can be divided into multiple processes depending on the desired machined shape. Angle of the rotational axis can varies depending on the machine and process. Degree of automation affects costs and production. What comes to machining properties, material utilization is not that great, and machine, tooling and labor costs are from moderate to high. Quality regarding the finished surface depends on multiple parameters such as machinability of the material, milling parameters, cutting fluids and using proper tools for the required machining. Achievable surface roughness in milling operations is between 0.2-25 µm. (Booker & Swift 2013, pp. 179-181.) Figures 6 & 7 below show 4-axis horizontal machining center capable of milling and drilling operations.

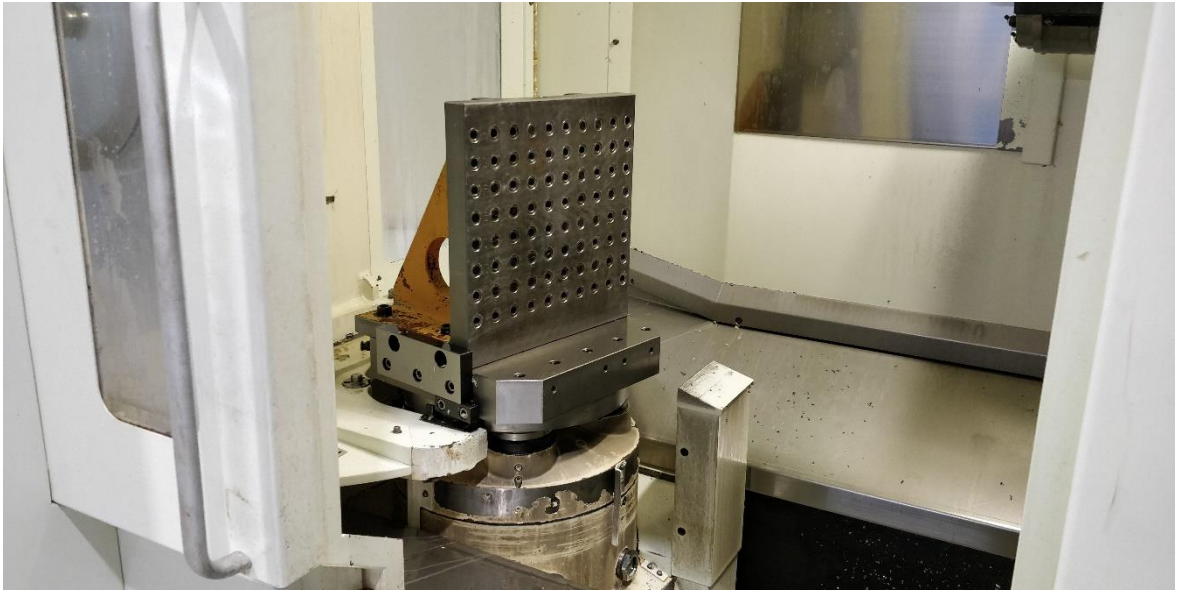**Figure 6.** 4-axis CNC machining center spindle and control panel.

Figure 7. 4-axis CNC machining center pallet.

CNC machines utilize computer-aided manufacturing (CAM) to create toolpaths for the machining based on cutting tool and material parameters set by operator. There might be some preset parameters for the machining based on the chosen tool and material, but adjustments can be made when necessary. Models can be created with computer-aided design (CAD) and imported to CAM by using common file formats. Many programs have combined CAD/CAM capabilities. (Evans 2016, pp. 295-296.) According to Mullen, machining times can be estimated from CAM simulations. CAM simulation takes different machining processes, tool changes and possibly other parameters into account when giving an estimate on the cycle time. (Mullen 2018.) Figures 8 and 9 below demonstrate turning process of a shaft in Edgecam 2018.

Figure 8. Workpiece and cutting tool in Edgecam 2018.
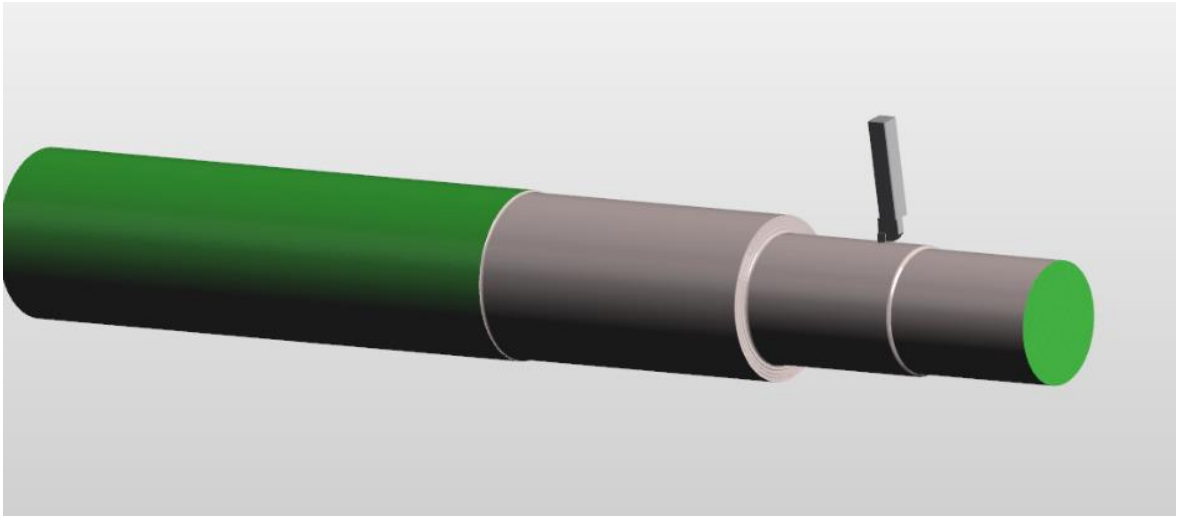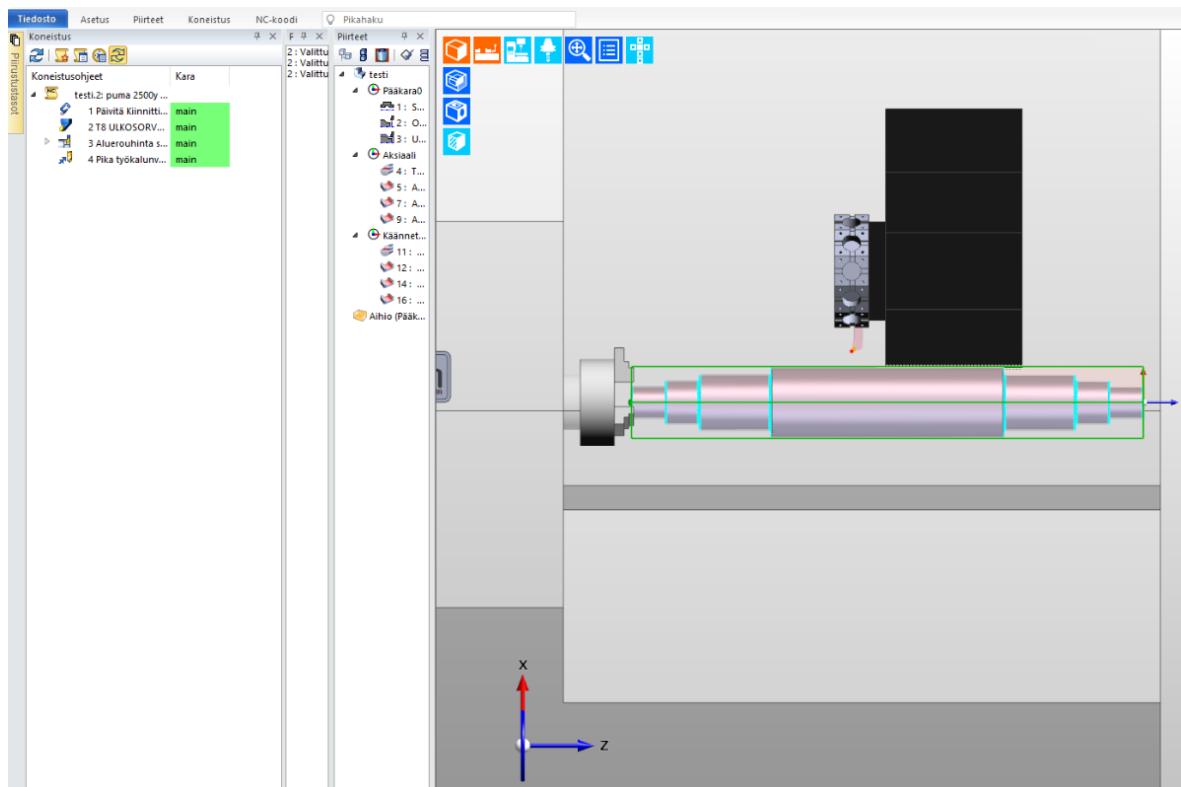

Figure 9. CNC lathe turret with cutting tool and workpiece with outline on original size in Edgecam 2018.

Figure 10 below demonstrates simulated toolpath for shaft turning with 3-axis lathe in Solidworks CAM in Solidworks 2020. Rough machining time estimation of around 81 minutes can be seen in Figure 11 below. Based on the simulation it doesn't machine flat

surfaces or threads and leaves few chamfers. More accurate estimations can be acquired with properly set up CAM simulations.

Figure 10. Shaft turning in Solidworks CAM in Solidworks 2020.

Figure 11. Rough machining time estimation in Solidworks CAM in Solidworks 2020.

Grinding is abrasive machining process which removes material from the surface using various abrasive particles bonded into different materials. In addition to particles and

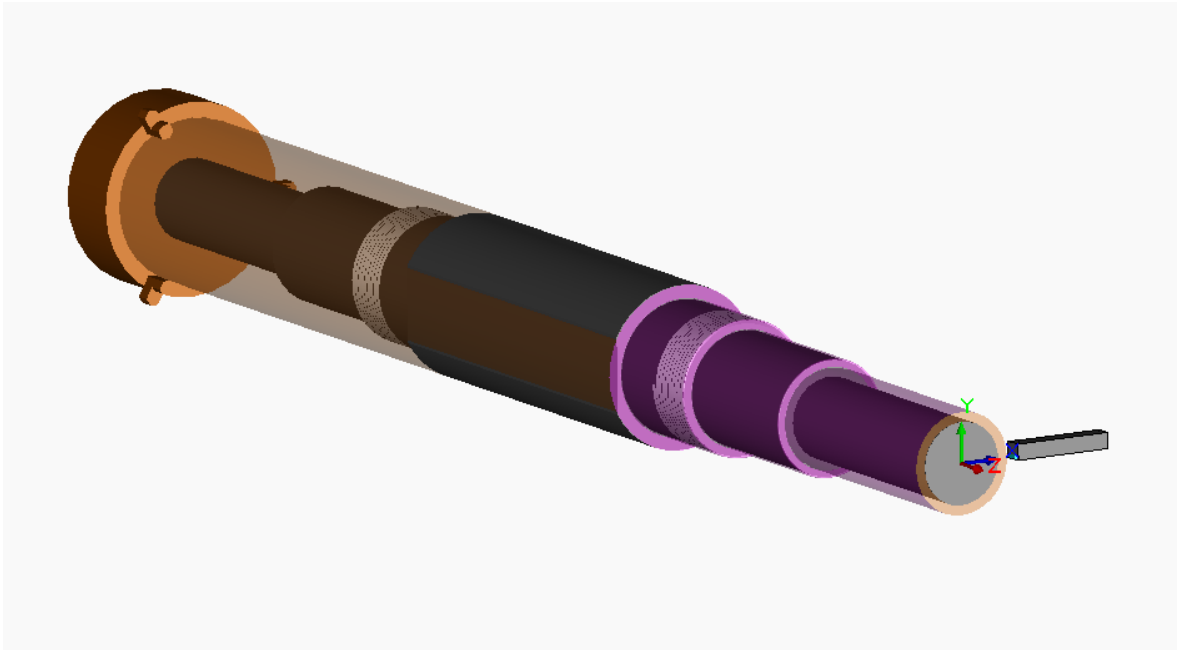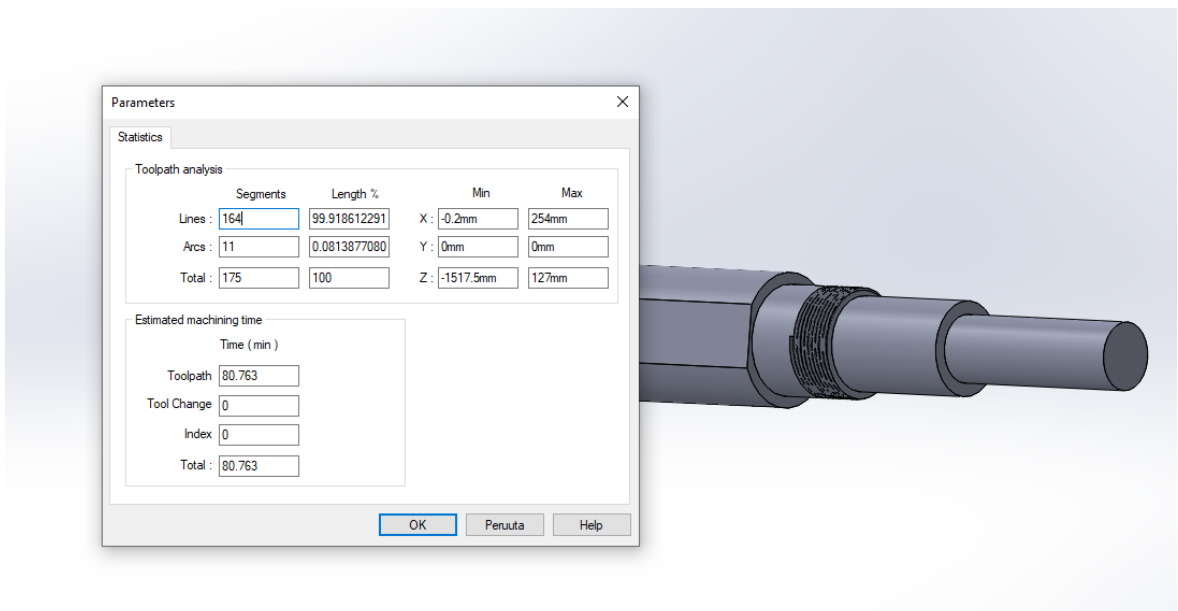bonding material used, grinding wheel parameters include grain size, wheel grade and structure. Optimizing these parameters affect the performance and durability of the wheel. There are limitations for the applicability of the grinding operations due to the shape of the workpiece. Flat surfaces can be ground by either vertical or horizontal surface grinding where either perimeter or face of the wheel is in touch with the workpiece. Cylindrical grinding rotates the workpiece and the grinding wheel in opposite directions in order to remove material from either internal or external contact surface. Alternative for cylindrical grinding would be centerless grinding where workpiece is suspended between regulating wheel, grinding wheel and possible support rolls. Belt grinding setup consists of looping belt infused with abrasive particles driven around pulleys. Lapping is similar process compared to surface grinding but there are few differences. Instead of using the grinding wheel, abrasive particles are in the lapping compound between the lapping tool and the workpiece. Lapping tool is moved on the surface in such way that all the lapped surface is subject to similar wear. (Groover 2019, pp. 547-549, 556-564.) Surface roughnesses for abrasive processes can be seen in Figure 12 below.

Process	Usual Part Geometry	Surface Roughness	
		μm	μ-in
Grinding, medium grit size	Flat, external cylinders, round holes	0.4–1.6	16–63
Grinding, fine grit size	Flat, external cylinders, round holes	0.2–0.4	8–16
Honing	Round hole (e.g., engine bore)	0.1–0.8	4–32
Lapping	Flat or slightly spherical (e.g., lens)	0.025–0.4	1–16
Superfinishing	Flat surface, external cylinder	0.013–0.2	0.5–8
Polishing	Miscellaneous shapes	0.025–0.8	1–32
Buffing	Miscellaneous shapes	0.013–0.4	0.5–16

Figure 12. Usual surface roughnesses for abrasive processes. (Groover 2019, p. 563).

Broaching is a material removal process where specific tool with multiple teeth in the shape of desired hole or surface is usually pulled through the workpiece. Broaching tool expands slightly with each tooth, cutting the desired shape closer to tolerances. Common broaching method is to pull the tool trough the workpiece. Other options are pushing the tool instead of pulling or moving the workpieces through the broach instead of other way around. (Groover 2019, pp. 491-492.) Typical tolerance for broaching is ±0.025 mm with a surface roughness of 0.2 µm (Groover 2019, p. 533).

1.5.2 Sheet metal processes

Applications for sheet metal processes in the rotor would be the lamination disks. Depending on the disk thickness, punching, blanking or fine blanking could be viable options for the squirrel cage holes. According to Booker & Swift, sheet metal processes would be feasible for thicknesses ranging from 0.1 mm to 13 mm. Sheet metal processes can be automated to different degrees and parameters regarding costs and production depend quite a lot on equipment. Fine blanking produces higher quality cuts with smaller tolerances compared to conventional blanking and piercing due to the clamping of the workpiece which restricts the movement. On the other hand, fine blanking requires higher quantities to be viable in economic sense. Surface roughness for sheet metal processes varies between 0.1 and 12.5 μm. (Booker & Swift 2013, pp. 118-121.)

Punch laser combination machines provide multiple sheet metal processes with high degree of automation. Depending on the machine there might be some bending and tapping functions in addition to punching and laser cutting. Cutting functions are improved by using fibre laser instead of CO_2 laser. Drawbacks of combination machines include machine costs and floor space requirements. Benefits of combination machine compared to stand-alone machines are improved productivity and optimized production. (Luminoso 2019) Required force for the punching can be calculated with multiplication between perimeter, thickness and shear strength of the material (Wilson Tool 2013).

Dimension and shape tolerances for 3 mm and thicker hot rolled steel plate are classified in standard SFS-EN 10029. SFS-EN 10029 sets the parameters on dimensions and shapes required from the plate. Thickness tolerances are divided into four classes, three of which are based on the amount of minus tolerance and one with symmetrical upper and lower tolerances. Flatness tolerance is the amount of permissible deviation from flatness which takes steel type, thickness and measuring length into account. (SFS-EN 10029 2011, pp. 6-9.) Manufacturers can provide additional guarantees for tighter tolerances than specified in the standards. In the Figure 13 below can be seen 5 mm thick lamination disk of Hardox 400 steel after first round of grinding. Due to the deviation in the dimensions, one side of the disk is ground, and other side is untouched. SSAB Hardox guarantee gives 5 mm thick plate thickness tolerances of min -0.3 mm, max +0.4 mm, and tolerance within plate of 0.5 mm.

Hardox flatness guarantee gives flatness of 3 mm per 1 m ruler for 5 mm thick Hardox 400 sheet and 5 mm per 1 m ruler for 5 mm thick Hardox 400 plate. (SSAB n.d.b. pp. 3-6.)

Figure 13. Hardox 400 disk after first round of grinding.

Surface of the ground disk can be seen in Figure 14 below. Machine used in the grinding process was 42 RB series (Timesavers) with configuration of abrasive belt and flap brushes. Grinding parameters affect quality of finished surface and machine should be adjusted accordingly. Conveyor speed of 0.2 m/min was used to get satisfactory finish on the disks. Burrs left from cutting operations are all on the same side which should be pointing upwards in the deburr process so the surface can be ground to tolerance.

Figure 14. Deburred and ground lamination disk.

1.5.3 Nontraditional cutting processes

There are multiple cutting and machining processes that use different methods to acquire the required shape. Processes can be divided roughly into mechanical, electrical, thermal, and chemical processes. Mechanical processes tend to erode the workpiece to acquire required shape. Electrical processes add or remove material from the workpiece using electrochemical reaction. Thermal processes cut material by focusing thermal energy to small area. Chemical machining processes use etching to machine the exterior of the workpiece which is not masked off. (Groover 2019, pp. 567-568.) Some approximate cutting times with different methods and thicknesses for single lamination disk can be seen in Figure 15 below.
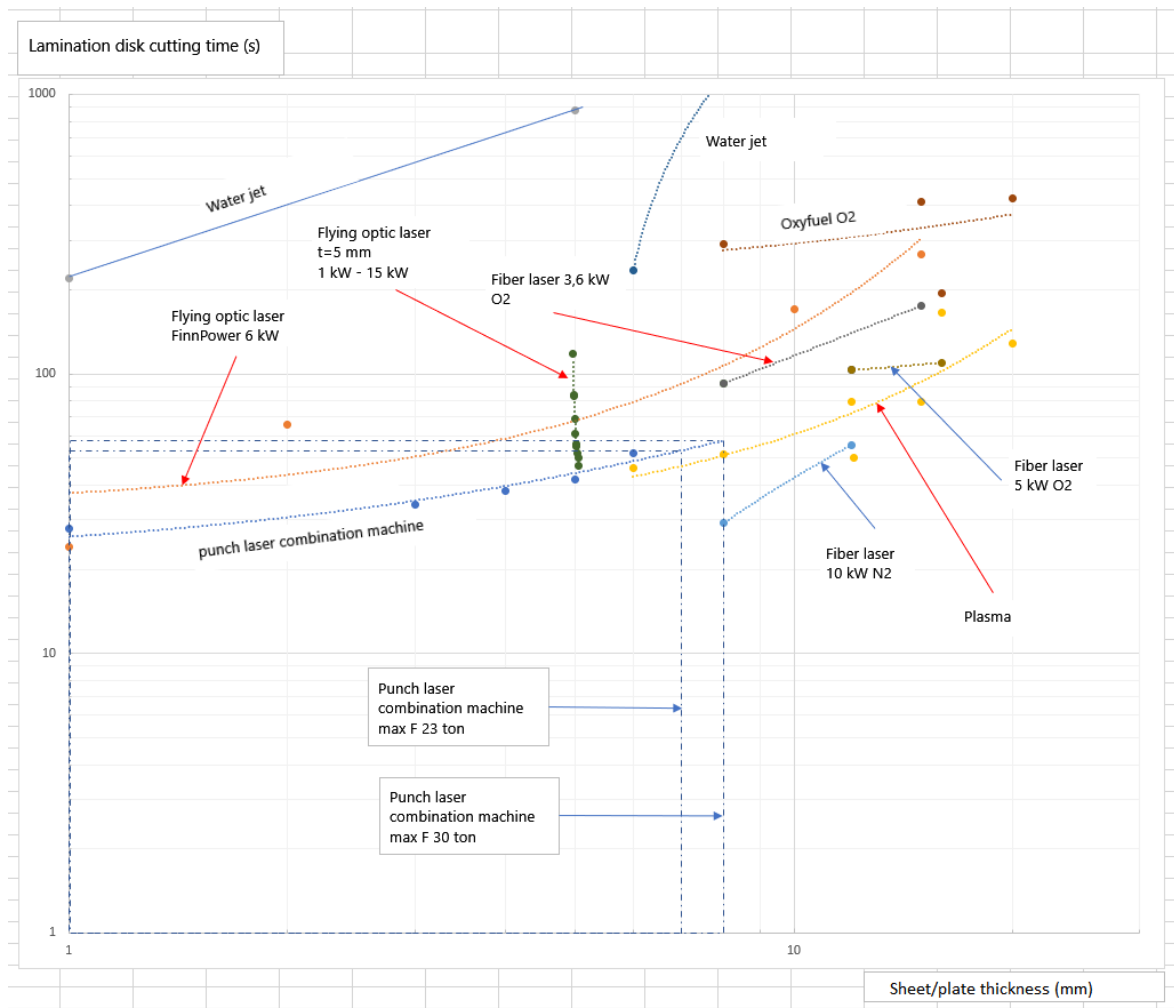
Figure 15. Approximate cutting times for single lamination disk with different methods and thicknesses.

Water jet cutting directs pressurized water through a small nozzle to cut variety of materials from cardboard to plastic. Process can be modified to abrasive water jet cutting by applying aluminum oxide, silicon dioxide or garnet particles to the stream after nozzle which enables the possibility to cut metals and minerals. Hydraulic pump generates cutting pressure trough the opening in the nozzle. Abrasive water jet cutting has slightly larger nozzle for higher flow rate, similar pressure and smaller standoff distance compared to normal water jet cutting parameters. On top of those, abrasive particles have parameters regarding type, grit size and flow rate. Abrasive water jet cutting is alternative to thermal cutting processes if properties resulting from heat input should be avoided. (Groover 2019, pp. 569-570.)

Laser-beam machining uses focused pulsed light to remove material. Lasers can be divided into CO_2 and solid-state lasers. Solid-state lasers can be further divided into different types one of which are fiber lasers which are growing in popularity due to benefits like cost, productivity, and accuracy over CO_2 lasers. Lasers can be used in different material removal operations such as cutting, drilling, and scribing. Desirable material properties for laser-beam machining include high light absorption and thermal conductivity and low reflectivity and thermodynamic properties regarding fusion and vaporization. Viable materials range from cloth to high strength steel. (Groover 2019, pp. 580-581.)

Plasma cutting is arc-cutting process where plasma stream, generated between tungsten electrode in the torch and anode workpiece, cuts through metal by melting it. Primary gas of nitrogen, argon, hydrogen, or combination of these is used to create the plasma stream. Torch directs the 10 000-14 000 °C plasma stream to the work piece and either water or secondary gas surrounds the plasma stream to improve the properties of the cut. Requirements regarding material include electrical conductivity. Plasma cutting process has high productivity, but the tradeoff is rough and damaged surface quality at the cut. (Groover 2019, pp. 581-583.)

Oxyfuel cutting process creates exothermic reaction between oxygen and metal with combination of combustion of fuel gases. Risen temperature by the combustion supports the material removal reaction between oxygen and metal. Ferrous metals are often cut with oxyfuel due to rapid oxidation of iron, but nonferrous metals are more oxidation resistant. Oxyfuel cutting of nonferrous metals can be improved by optimizing the heat of combustion or introducing additives into the oxygen stream to improve oxidation of the metal. Oxyfuel cutting process can be done manually for some rough cuts or automatically with numerical control where cutting speed and accuracy are improved compared to manual cutting. (Groover 2019, pp. 583-584.)

1.6   Coating processes

Copper alloy squirrel cage has higher electrical conductivity compared to lamination steel which keeps the current flow constrained without needing any insulation around the squirrel cage (Boulter et al. 2014, p. 11). Efficiency and temperature can be improved in the rotor by insulating the lamination disks from each other which reduces axial currents from the main

magnetic field from flowing in the rotor (Boulter et al. 2014, pp. 149-150). Electrical insulation coating on the lamination disks prevents interlaminar eddy currents in the lamination stack (Kliman & Toliyat 2004, p. 280). Depending on the steel there might be coating pre-applied on the steel by manufacturer. ASTM A976-1997 standard has some classifications for electrical steel coatings. Coatings range from C-0 to C-6 and each classification has specific properties to accommodate welding or annealing among other things. (Boulter et al. 2014, pp. 149-150.)

Black oxide coating is conversion coating technique that creates thin magnetite layer on the workpiece by oxidizing salt. Thickness of the black oxide layer derives from the duration of the heating process and temperature where longer process or process at higher temperature creates thicker magnetite layer. Thickness of black oxide coating of AISI 1015 steel ranges around 16 μm to 20 μm with process time ranging from 30 min to 90 min and temperature ranging from 100 °C to 200 °C. Gloss of the surface decreases with the duration of the process. (Palupi, Riandadari & Sakti 2020, pp. 250-253.) Lamination disk with black oxide coating can be seen in Figure 16 below next to uncoated one. Material for both is Hardox 400 and thickness is 5 mm.

Figure 16. Lamination disks with and without black oxide coating.

Test disks used in measuring electrical resistivity of black oxide coating were grinded so there wouldn't be any jagged edges pushing through the coating layer. Three disks were coated, and three disks were without finish. There were three setups of for the disks, one had all six disks alternating between coated and uncoated while second setup had three coated disks on top of each other and third had three coated disks with 0.3 mm electrical steel sheet between the disks. Setups were measured with compression of 0 kN and 100 kN. Alternating disk setup had resistance of 125 Ω with 0 kN and 0.2 Ω with compression of 100 kN. Stack of three coated disks had resistance of 93 Ω with 0 kN and 0.2 Ω with compression of 100 kN. Coated disks with electrical steel between disks had infinite resistance at 0 kN and 0.5 Ω at 100 kN. At compression the resistance dropped significantly. There is possibility that there would be some small rough edges even after grinding which would have pushed through the coating layer at compression and ignored the resistivity of the coating. Possible improvements for the black oxide coating could include smoother grinding or thicker black oxide layer.

Berylliym oxide powder can be used in metal finish which offers thermal conductivity with electrical resistivity (AOTCO 2015). According to American Beryllia Inc., thermal conductivity of beryllium oxide at room temperature would be 275 W/mK with electrical resistivity of 10^{16} Ωcm. Compared to aluminum oxide, beryllium oxide has lower mechanical strength, 25% lower density and ten times higher thermal conductivity. (American Beryllia Inc. n.d.)

Aluminum oxide (Al_2O_3) also known as alumina has some beneficial properties as a coating. Coating can be applied by various thermal spraying processes. Average thickness of single coating layer was 3.0 ± 0.5 µm for atmospheric plasma spraying (APS) and 2.8 ± 0.5 µm for detonation gun spraying (DGS). Coating thickness of up to 2 mm can be achieved with APS. Electrical resistivity of alumina coating is lower compared to bulk alumina and varies depending on the powder, deposition processes and parameters used. Electrical resistivity of alumina coating is in the range of 10^7-10^{12} Ωm. Thermal conductivity of alumina coating varies depending on the porosity level of the coating. Thermal conductivity of 1 mm thick coating was 3.3 ± 0.8 W/m·K with porosity of $10.0 \pm 2\%$ for APS and 4.0 ± 0.8 W/m·K with porosity of $3.0 \pm 0.6\%$ for DGS. (Azarmi et al. 2017, pp. 15392-15393, 15397-15400.)

Polytetrafluoroethylene (PTFE), commercially known as Teflon, is fluoropolymer with high thermal resistance. PTFE is used in various fields due to its various properties. Chemical inertness, low surface energy and high thermal resistance can be used in applications from cookware coating to self-lubricating ball bearings. PTFE coating process uses emulsion to attach PTFE particles to the surface. Fluorine compounds can be used to improve the coating process. (Dhanumalayan & Joshi 2018, pp. 247, 256-257.) PTFE coatings have continuous operating temperature up to 290 °C with melting point at 327 °C. Thermal conductivity of PTFE coating is 0.25 W/m·K with dielectric strength of 18 V/µm. (Matrix Coatings n.d.) PTFE coated lamination disk can be seen in Figure 17 below. Coating was done on the ground disk without using primer before coating. Thickness of the PTFE coating is 30 µm.

Figure 17. PTFE coated lamination disk.

Perfluoroalkoxy alkanes (PFA) are fluoropolymers with similar properties to PTFE. PFA is optically transparent, chemically resistant material which can be used in tubing applications for corrosive processes. Electrical and thermal and mechanical properties are similar

compared to PTFE. (EMERSON 2017, pp. 1-3.) According to iPolymer, PFA coating cost factor could be two to three times higher compared to PTFE coating (iPolymer 2018).

Diamond-like carbon (DLC) coating possesses beneficial properties, among which, electrical resistivity and thermal conductivity (Imai et al. 2004, p. 2454). According to Annaka et al., hardness and protective properties of the DLC film can be altered by modifying the hydrogen content. Common processes to create DLC film on the coated piece include chemical vapor deposition (CVD) and physical vapor deposition (PVD). There are multiple CVD processes, among which plasma CVD which has advantage of coating 3D structures. (Annaka et al. 2020, p 2.) Approximately 40 nm thick DLC film created with plasma CVD with deposition time of 360 s had average resistivity of $10^{14}\,\Omega$m (Imai et al. 2004, p. 2456).

1.7   Research problem and questions

Laminated squirrel cage induction machines have high efficiency but are relatively difficult to manufacture compared to solid rotor induction machines and tend to lack properties for high-speed applications. This thesis aims to answer questions such as how improve manufacturability of laminated squirrel cage rotor and how to improve mechanical strength of the rotor to withstand high-speed applications?

1.8   Aims and objectives of the thesis

Aim of the thesis is to explore possible options for cost effective manufacturability of laminated squirrel cage rotor. Objectives to achieve the aim consist of researching the current direction of rotor manufacturing, reviewing possible options in terms of materials and methods, and combining the obtained information into package of possible options in terms of manufacturability.

1.9   Framing

This thesis concentrates on laminated squirrel cage rotor in terms of materials and manufacturability. Squirrel cage rods and end rings are not focused on too much. Other induction rotor constructions might be investigated for comparison.

2   METHODS

Method for acquiring information regarding manufacturability of induction machine is combination of literature review, meetings, and interviews. Objective is to gather information from different sources regarding construction, materials, tolerances, manufacturing methods, costs, machining times, surface coating, strength analysis and cam simulations. Sources include different research papers, articles, patents, websites, manufacturers, and current constructions.

2.1   Design process

Design of the rotor and potential materials are quite volatile in terms of changes due to nature of the project. New options might be discovered, or old options reconsidered which turns the wheels on other groups. Design process itself is iterative loop of concurrent engineering where preliminary structure and materials are designed according to requirements for the induction machine and those features are examined from the viewpoint of manufacturing. Feedback from manufacturing options loops back to design team and changes can be made depending on the options and the modified design can be reviewed again.

2.2   DFMA

Design for manufacturing and assembly (DFMA) is systematic design technique which optimizes the design process to reduce costs and manufacturing times. DMFA can be divided into design for assembly (DFA) and design for manufacturing (DFM). DFA optimizes the assembly process by reducing and redesigning parts which streamlines the assembly process. Tradeoff for applying DFA process is increased complexity which may diminish or negate the gained benefits. DFM optimizes the manufacturing process to reduce the cost of the parts by material selection, reducing number of processes and using standard parts. (Naiju 2021, pp. 1-2, 5.)

2.3   Manufacturability

This thesis reviews the options regarding manufacturability of different parts in terms of materials, methods, machine costs, machining times, manufacturing costs, quality, and

tolerances. Combination of these factors might form some understanding manufacturability of the rotor.

3   MANUFACTURABILITY OF COMPONENTS

Rotor parts are divided into four main components which are reviewed for required features and possibilities in terms of manufacturing. Approximate model of the assembled rotor can be seen in Figure 18 below. Main baseline dimensions for the rotor include length of the shaft being 1500 mm, length of the lamination stack being 400 mm with diameter of 254 mm.
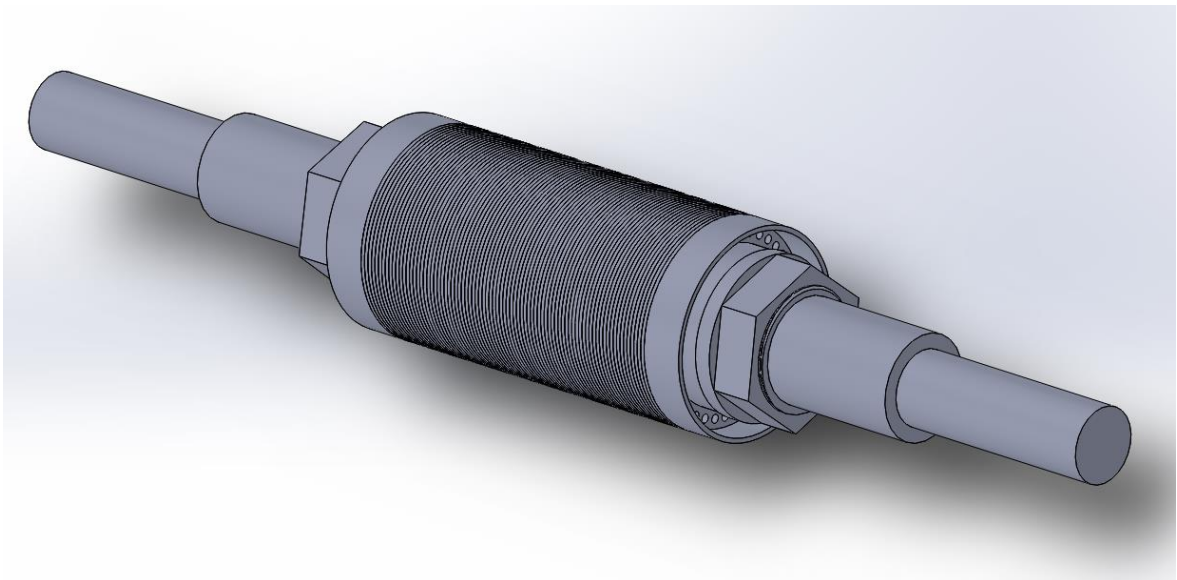

Figure 18. Approximate model of the assembled rotor consisting of shaft, lamination disk stack, end disks and end disk nuts.

3.1   Shaft

Material for the shaft is structural steel S355. Features in the shaft include few shoulders, couple threads, couple milled surfaces and surface finishes for the magnetic bearings. Shoulders are for magnetic bearing disks, which restrict axial movement in the bearings, and flexing end disks which restrict movement and bending in laminate stack. Threads are for the end disk nuts which lock the flexed end disks in place. There would be two milled surfaces opposite sides of each other to restrict movement in lamination stack. Magnetic bearings at the ends of the shaft have requirements regarding surface finish. Shaft can be cut from round bar with band saw and machined in multifunction lathe. Approximate model of

the shaft can be seen in Figure 19 below. Dimensions and features on the shaft are rough estimates and can be subject to change.
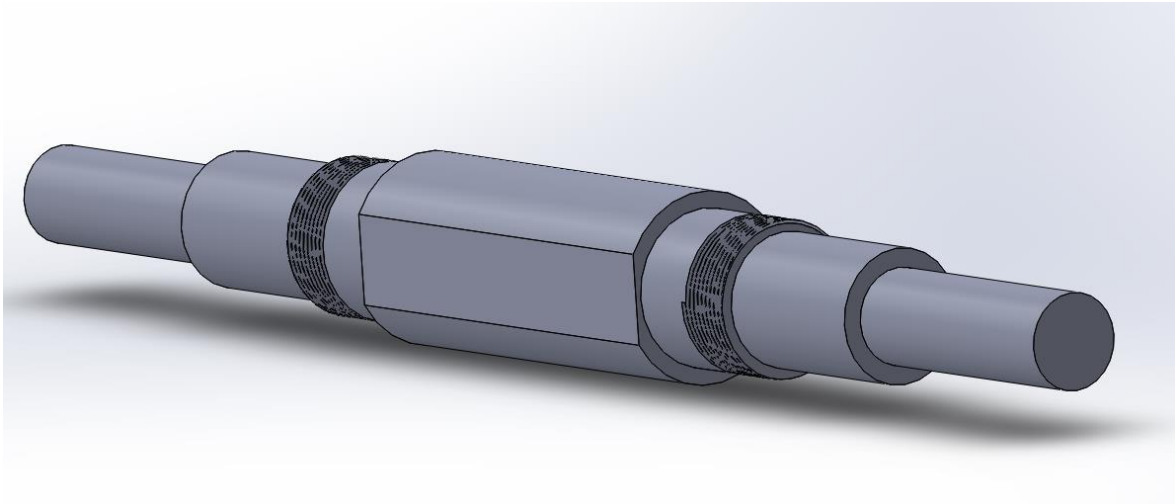

Figure 19. Approximate model of the shaft.

Due to relatively simple shapes turning, milling, and boring for shaft, end disk and end disk nut could be done with multi-axis mill-turn machine. According to Cope, 3-axis mill turn would have xz & c-axes, where c-axis rotates the work piece and xz-axes move the spindle. There are limitations for milling flat surfaces with 3-axis mill-turn and additional y-axis for the spindle would help with machining flat surfaces in the middle of the workpiece. (Cope n.d.) Y-axis in the 4-axis mill-turn would be suitable for machining the flat surfaces for the shaft and end disk nut, although end disk nut flat surfaces could be done with 3-axis mill-turn. According to Bhattacharyya and Doloi, normal tolerance for turning would be between ±50-12.5 μm while normal surface roughness for turning would be between 6.3-0.4 μm. Cutting speed for conventional turning varies depending on different parameters but generic cutting speed listed is 76 000 mm/min. (Bhattacharyya & Doloi 2020, pp. 15-17.) Machining times and manufacturing costs can be estimated from the designed model for the shaft.

3.2 Disk

Baseline material for the disk is S960. Features in the disk include otherwise circular hole in the middle with two flat surfaces opposite sides of each other as counterpart for the shaft, and undefined number of holes with oval shape. Desired surface finish regarding the disks includes flat, deburred, and coated surface that stacks straight and improves electrical

properties of the rotor. Depending on the thickness disks are cut from either sheet or plate. Options regarding cutting methods include waterjet, flame, plasma, and laser cutting as well as punching, blanking and fine blanking, or combination those of processes. If the lamination disks would be thinner, required force for the fine blanking would be lower and number of disks would be higher. With the baseline parameters of 5 mm thickness of S960, capabilities of fine blanking fall off. That combined with relatively low yearly output of the rotors makes it hard to justify equipment investments for it. Broaching the middle hole is an option to get the dimensions to tolerances for the shrink fit. Cost-effectiveness and required thickness of the disks are major parts in choosing optimal process for manufacturing.

Deburring of the rough edges after cutting and grinding of the disk could be done with sheet metal processing machine where the parts are transported and machined on conveyor belt through modular set of rollers, brushes, and discs. Other option for the grinding could be double disc grinding machine but that would probably require separate deburring and capacities of the machine may become an issue. Lamination disks should be separated with electrically insulative layer to improve magnetic and mechanical properties. Options for the layer include thin sheet of electrical steel or mica paper, black oxide, beryllium oxide, aluminum oxide or diamond-like carbon coatings, adhesive layer of epoxy resin or something similar which could withstand the heat. Methods for applying the coating material include roll coating, chemical coating, physical vapor deposition and electrophoretic deposition depending on the coating material. Approximate model of the 5 mm thick disk can be seen in Figure 20 below. Dimensions and features on the disk are rough estimations and can be subject to change.
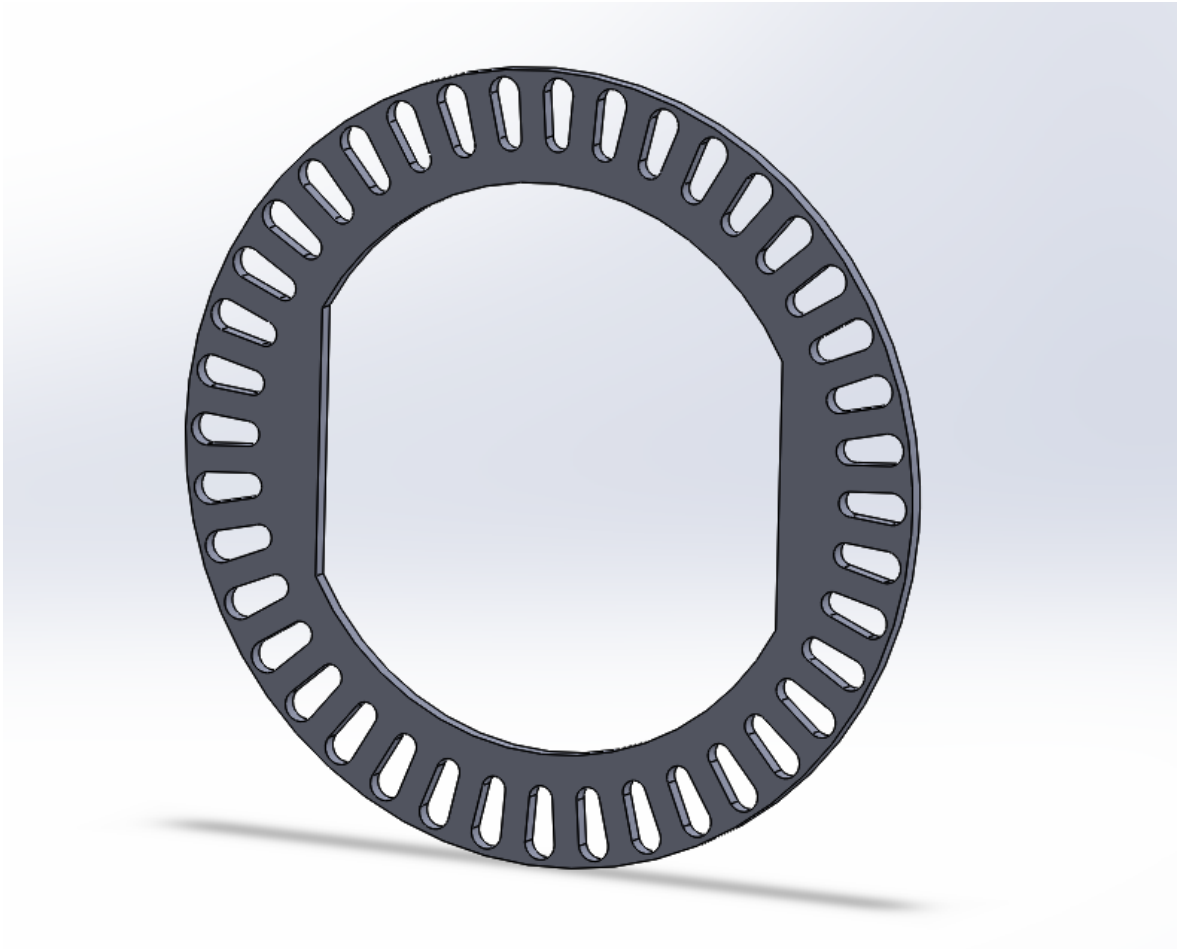
Figure 20. Approximate model of the 5 mm thick disk.

Depending on the required thickness, disk can be cut from sheet or plate. Cutting methods for thinner disks include blanking, fine blanking, punching, laser, and waterjet processes while thicker disks can be cut with laser, plasma, oxyfuel and waterjet processes. Waterjet, oxyfuel and plasma cutting can be left out due to unfavorable properties regarding cutting speed or quality. Material properties and thickness of the disk determine cutoff thickness between stamping processes and laser cutting. Deburr and grinding operations improve stacking properties as well as surface area between laminations. Deburring and grinding can be done with multifunction sheet metal processing machine. For the coatings there are few options. Precoated thin sheets of electrical steel where there is bonding varnish pre-applied on the surface from the factory before any machining processes. Another option would be lamination stack epoxy adhesives that can be applied on the disks. One option could be applying some insulation coating via electrophoretic deposition where the parts would be transported on a monorail and submerged for the coating.

3.3   End disk

Baseline material for the end disk is Inconel alloy due to mechanical properties at high temperatures. Purpose of the end disk is to keep compression on lamination stack and house the squirrel cage end ring and rod ends. Features of the end disk include groove, and holes in the groove for the squirrel cage, hole in the middle for the shaft and concave shape in the middle which acts as a spring under load. Approximate model of the end disk can be seen in Figure 21 below. Dimensions and features on the end disk are rough estimates and can be subject to change.

Figure 21. Approximate model of the end disk.

End disk can be cut from a round bar or a thick plate depending on the dimensions. Cutting it from a round bar with band saw would minimize the material waste but availability and transportation of quite large diameter round bar is inferior to plate. Thick plate of Inconel can be cut with powerful laser but plasma cutting would be better option. Surface quality of the cut would not matter too much if shape of the end disk is acquired by forging. Basically, the groove and concave shape of the end disk could be turned in lathe but amount of material being removed and baseline material being Inconel makes forging a better option. Finishing

turning and boring for the outer and inner surfaces and holes for the squirrel cage rods can be done in mill-turn.

3.4   End disk nut

End disk nuts are made out of S355. Purpose of the nuts is to keep the end disk in place so there would be tension in the lamination stack. Features of the nuts include hole with thread for the shaft and hexagonal surfaces on the outside. Options regarding manufacturing methods for nuts include forging, turning, milling, and boring which can be done in multi-axis mill-turn from a round bar cut to length with band saw or circular saw. Approximate model of the end disk nut can be found in Figure 22 below. Dimensions and features on the end disk nut are rough estimates and can be subject to change.
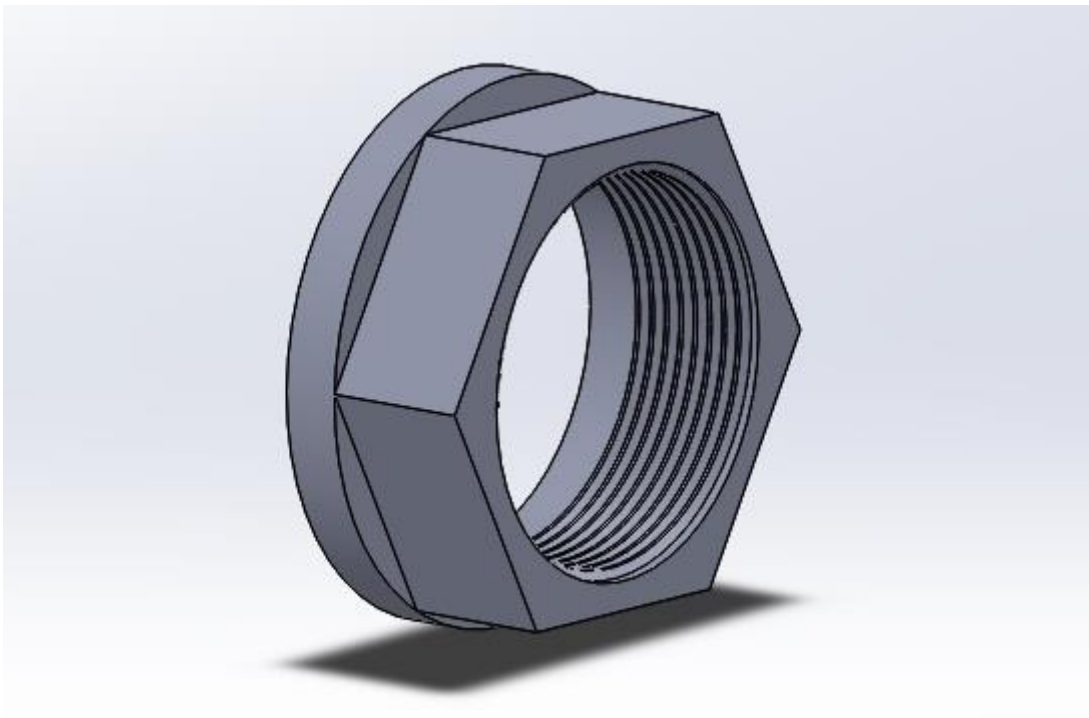
Figure 22. Approximate model of the end disk nut.

3.5   Assembly of the rotor

Rotor assembly can be done vertically or horizontally. One end disk, copper ring and end disk nut are preassembled on one end of the shaft. Lamination stack with copper rods is assembled on temporary smaller shaft in preparation for shrink fit. Balancing of the rotor is done at relatively low speeds due to limitations in capabilities of the machinery. In order to

replicate regular working conditions during the low-speed balancing, copper rods should be forced to the outer edge in the laminations. This can be done with spring pins installed under the copper rods in the lamination stack. There are couple options regarding the shrink fit between laminate stack and the shaft. Shaft can be cooled with dry ice, cooling bath or constant temperature chamber to get large enough thermal contraction for the shrink fit. Constant temperature chamber could be viable to -50 °C but problems might arise in dimensional capacity of the chamber due to the size of the shaft being around 1500 mm long. Temperature and methods to acquire it depend on the shrink fit requirements. Another option is to heat lamination stack along with the copper rods to get large enough thermal expansion for the shrink fit. Combination of those is also possibility. Lamination stack with the copper rods is installed on the shaft, against the preassembled copper ring, end disk and end disk nut. Assuming that lamination stack is stacked straight, it should fall right into the shaft guided by the flat surfaces. Top copper ring and end disk along with the end disk nut are installed and axial pressure from the end disks is applied, during which upper end disk nut is tightened. Copper rods can be soldered, brazed, or upset forged into the copper disks. Outer surface of the rotor is turned in lathe to improve the surface quality and optimize the thickness between squirrel cage and rotor surface.

Selected stages for induction machine squirrel cage rotor in terms of materials and manufacturability are listed in Table 1 below. Machining times and manufacturing costs are approximations based on the model and process used.

Table 1. Manufacturing options regarding rotor parts

Part	Materials	Manufacturing method stages	Main parameters affecting machining times and manufacturing costs	
Shaft	S355	Cutting	tooth design, band speed, feed rate	[b]
		Turning	diameter, length, feed, cutting speed	[a]
		Milling	approach distance, length, width, depth, feed rate	[a]
		Grinding	speed, depth of cut, width of path	[a]
Disk	S960	Cutting	depends on the cutting method	
		Deburring		

Table 1 continues. Manufacturing options regarding rotor parts

		Grinding	speed, depth of cut, width of path	[a]
		Coating	depends on the coating	
		Broaching		
End disk	Inconel	Cutting	depends on the cutting method	
		Forging		
		Turning	diameter, length, feed, cutting speed	[a]
		Drilling	workpiece thickness, feed rate, approach distance	[a]
		Boring	diameter, length, feed, cutting speed	[a]
End disk nut	S355	Cutting	tooth design, band speed, feed rate	[b]
		Turning	diameter, length, feed, cutting speed	[a]
		Milling	approach distance, length, width, depth, feed rate	[a]
		Drilling	workpiece thickness, feed rate, approach distance	[a]
		Boring	diameter, length, feed, cutting speed	[a]

[a] (Groover 2019), [b] (LENOX n.d., p. 5)

4   ANALYSIS & DISCUSSION

There are number of options for manufacturing processes for each part and depending on the materials and dimensions, different processes have benefits and drawbacks. Some parts are more straightforward than others and parts like shaft and end disk nut can be machined in single 4-axis mill-turn whereas there are parts like disk or the end disk where there are no obvious answers for the optimal manufacturing method.

4.1   Shaft

Shaft can be cut to length by band saw since diameter is rather large for circular saw. Machining of the shaft can be done in the multi-axis mill-turn. Depending on the machine, there are options for grinding heads for the spindle so turning of the shoulders and threads, milling of the flat surfaces, and grinding of the surface for active magnetic bearing can be done with 4-axis mill-turn. Designed material for the shaft is S355 which is relatively cheap and easy to machine compared to higher strength materials. Challenges with the shaft are probably related to the dimensions. Length of the shaft is quite large which requires machinery with enough capability and due to the long and relatively thin shaft, vibrations should be taken into account in the turning process.

4.2   Disk

Cutting method for disk depends quite a lot on the thickness and material. Sheet metal processes such as punching or fine blanking are viable up to certain hardness or thickness of the material where the capabilities of those processes are not feasible anymore. Fine blanking capabilities depend on the thickness and required force for the blanking to work. Decreasing the thickness of the disk improves the capabilities of fine blanking due to the increased number of disks for each rotor and less force needed from the machine. Fiber laser seems to be viable option when capabilities of the sheet metal processes fall off. Middle hole could be broached to get better quality surface for the shrink fit. Depending on the cutting process and requirements regarding surface quality, grinding and deburring can be done with multifunction grinding machine. Grinding quality should be decent to avoid any rugged edges penetrating the coating layer or electrical steel and defeating the purpose of the insulation. Insulation coating limited on the area around the squirrel cage bars on the outer

rim of the lamination disks could be sufficient due to the currents being located around the squirrel cage bars. On other hand it may be easier to just coat the whole disk instead of limiting the insulation area. After the coating process, middle hole of the disks should be broached to get sufficient quality and tolerances for the shrink fit since the surface quality is result from laser cutting combined with possible coating.

Thin coating layer for the disk should have electrically resistive and thermally conductive properties. There are significant rotational forces at high speeds and layer between the laminations should be hard enough to withstand the bending. Some potential options for thin and hard coatings include beryllium oxide, aluminum oxide, polytetrafluoroethylene (PTFE), perfluoroalkoxy alkanes (PFA) and diamond-like carbon coatings which should have varying amounts of electrical insulation and the insulation layer thickness would double if both sides were coated in the process. These coatings have varying amounts of thermal conductivity, electrical resistivity, and corrosion resistance. Black oxide coating was considered and tested but the results for the black oxide coating were less than optimal since the electrical insulation of the coating dropped when axial pressure was applied on the disks. Consensus was that the surface of the black oxide disks wasn't smooth enough and small shards would have penetrated the oxide layer which defeats the electrical insulation and purpose of the layer. Potentially black oxide layer could work if the surface would be ground smoother, oxide layer could be thicker or if the construction would be redesigned where there wouldn't be axial pressure on the lamination disks.

Another option considered was adding thin sheet of insulative material between the laminations. Mica sheet, found in microwaves and such, has electrical and thermal insulation properties but the concern with mica sheet is the bending under pressure. Another option was to add thin sheet of electrical steel between the lamination disks. Depending on the design and rotation speeds mechanical strength of thin sheets of electrical steel might not be enough as standalone lamination stack but they could work as insulative layer between thicker lamination disks. There are same concerns with electrical steel insulation as was with black oxide coating where rugged edges on the surface of the disks would penetrate the surface negating the insulation properties. Possible solutions include double layer electrical steel or smoother grinding of the surface. One option considered was adhesive layer between the laminations. In addition to being an insulation layer, it would increase the mechanical

strength between the laminations and against bending. It could be viable option if the bending of the adhesive layer is not too much. One reason against the adhesive layer between the laminations was the estimation of the produced heat in the rotor. Estimates were upwards from 200 °C which were later lowered to 120 °C at the rotor surface due to estimated efficiency of the laminated squirrel cage design.

4.3   End disk

End disk material being thick piece of Inconel, plasma cutting the disk from a plate seems to be best course of action. There are few options for shaping the Inconel disk to required form. Disk could be machined in multi-axis turn mill, but the machinability of Inconel is not that great and if mechanical functions of the end disk could be achieved with softer material traditional machining could be viable option. Forging and machining is one option where Inconel disk would be forged in closed die for the required shape. Surfaces and holes could be machined in multi-axis turn mill after forging.

Designed feature of end disk acting as a plate spring to keep lamination stack tight may have some drawbacks depending on dimensions of the shaft. In the case of thick shaft relative to the diameter of the rotor, there might not be enough room for the plate spring functions in addition to housing the squirrel cage end ring. Thicknesses in the end disk depend on the mechanical strength requirements for housing the squirrel cage end ring. Design for the end disk should be revised in order to acquire sufficient flex from the center of the end disk and compression from the outer rim of the end disk to the lamination stack. Other choice is to move away from the plate spring function and focus on more traditional design for squirrel cage induction machines.

4.4   End disk nut

End disk nut can be cut from round bar with either circular saw or band saw and machined in multi-axis turn mill. Outer surface can be turned, head for the nut can be milled whether it is hexagonal or something else. Starting point for boring can be drilled and threads can be bored at the inner surface. Following DFA methods, end disk nut could be integrated into the end disk itself which would reduce one part and few processes from the rotor manufacturing. Problem would probably arise in assembly process where end disk and nut being single piece, pressure could not be applied enough over the friction resistance between end disk and lamination disk to tighten the lamination pack for the plate spring structure to

work. End disk and nut being separate pieces allows pressure to be applied on the end disk itself and there would not be any friction resistance while tightening the nut. Another problem with end disk nut and end disk being combined piece would be copper bars of the squirrel cage. In order to tighten the end disk, there can't be any copper bars inserted at the time due to the relative rotation of the end disk compared to stationary lamination pack. That would require lining up the holes of end disk and lamination stack and insertion of copper bars afterwards. It could have potentially worked since flat surfaces on shaft and lamination disks line up the squirrel cage holes in the lamination stack and threads for the end disk could have been machined in a way that sufficient axial pressure is applied, and holes would line up with the lamination stack. Problem with that comes with varying thickness of lamination disks where the exact location of the contact surface between end of lamination stack and end disk is not constant. Also, assembly order would change slightly with installing copper rods after tightening of the lamination pack which could surface more problems with installing spring pins used to position copper rods for the balancing. It would be preferable to use separate pieces for the end disk and nut.

4.5   Assembly

Assembly of the rotor depends quite heavily on the chosen construction. With the current symmetrical construction, assembly process starts with assembling the end disk and end disk nut on one end of the shaft which works as backstop for the lamination stack later on. Shrink fit for the lamination stack can be done with either heating the lamination stack or cooling the shaft depending on the circumstances or both. It should be light shrink fit so it shouldn't matter too much. Due to the flat surfaces on shaft and lamination disks they should line up automatically but to get end disks to line up with lamination stack probably requires the copper rods which are inserted into the end disk holes. Copper rods should be forced into the outer surface of the lamination stack holes for balancing of the rotor. This can be achieved by installing spring pins under the copper rods. Installation of the spring pins can be done before heating of the lamination stack by partially building the stack and installing the pins at specific intervals. Another option would be to install the pins by pushing them at place from the ends of the lamination stack. Before the shrink fit attaches itself, end disk and end disk nut should be assembled, and pressure should be applied on the end disk in such a way that end disk nut can be tightened to keep the pressure on the lamination stack. After that, copper end rings for the squirrel cage can be installed and upset forged into the copper

bars. Surface of the rotor is machined in lathe or grinded to improve the surface quality, which also reduces friction coefficient, and optimize the thickness between squirrel cage and rotor surface.

4.6 Comparison to current rotor design

According to approximate analysis by Chazal et al., tesla Model S 60 uses 225 kW, 15 000 rpm induction motor with 74 bars in the squirrel cage. Squirrel cage slots are narrow and tall as can be seen in Figure 23 below and working temperature would be 150 °C. Cooling of the rotor is arranged with water jacket on the outside and spiral groove inside the rotor shaft. Material choice for the squirrel cage is pure copper which has advantages and drawbacks. With better conductivity pure copper has reduced losses compared to aluminum rotor and thus better efficiency but manufacturing is more expensive and copper rotor weights more compared to aluminum one. (Chazal et al. 2020, pp. 1-2, 5-6.)
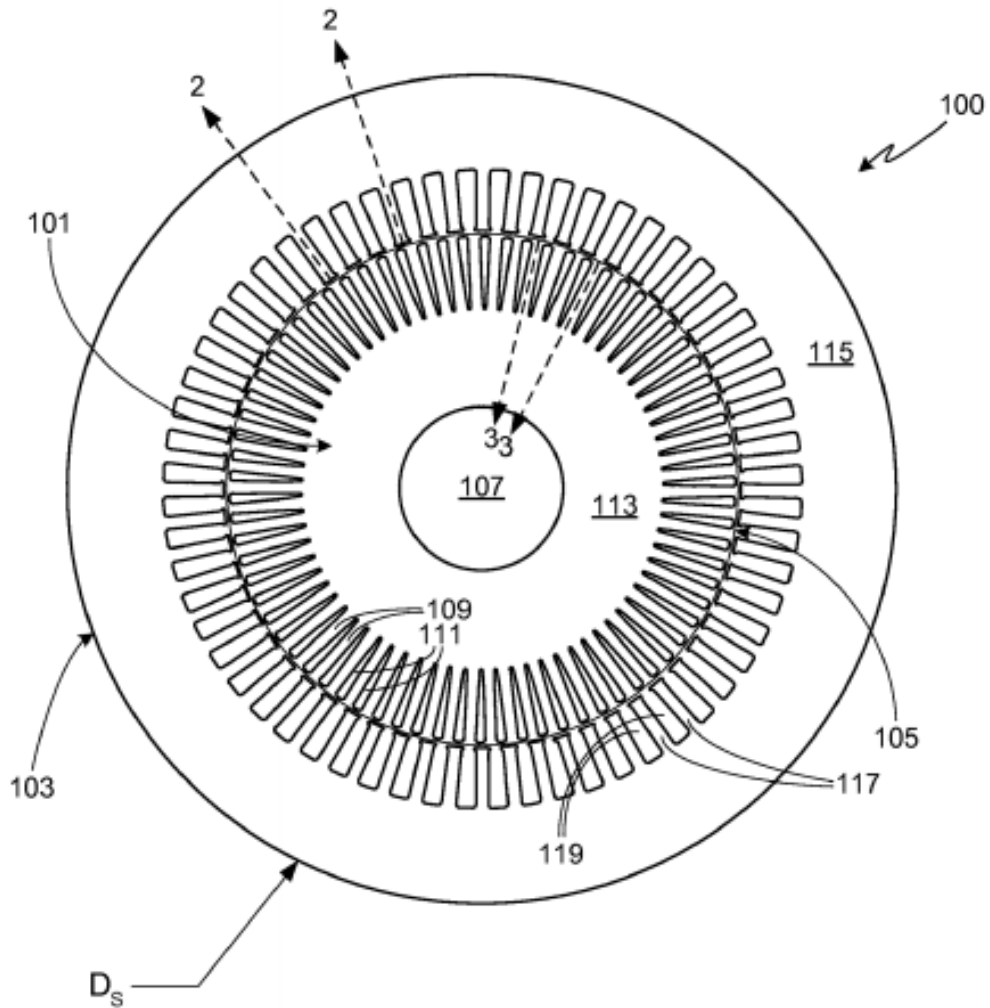
Figure 23. Tesla patent for induction motor lamination design (Pat. US 8,154,167 B2 2012, p. 1).

Audi e-tron uses two asynchronous squirrel cage induction motors with rotation speed of 15 000 rpm and peak power ranging from 90 kW to 140 kW per motor depending on the variant. Rotor consists of 0.35 mm thick electrical sheet laminations with adhesive coating. Squirrel cage is die-cast aluminum with 58 rods. Cage ring of the rotor feature curved fan blades which can be seen in Figure 24 below. (Ardey et al. 2019, pp. 9, 14-16.)
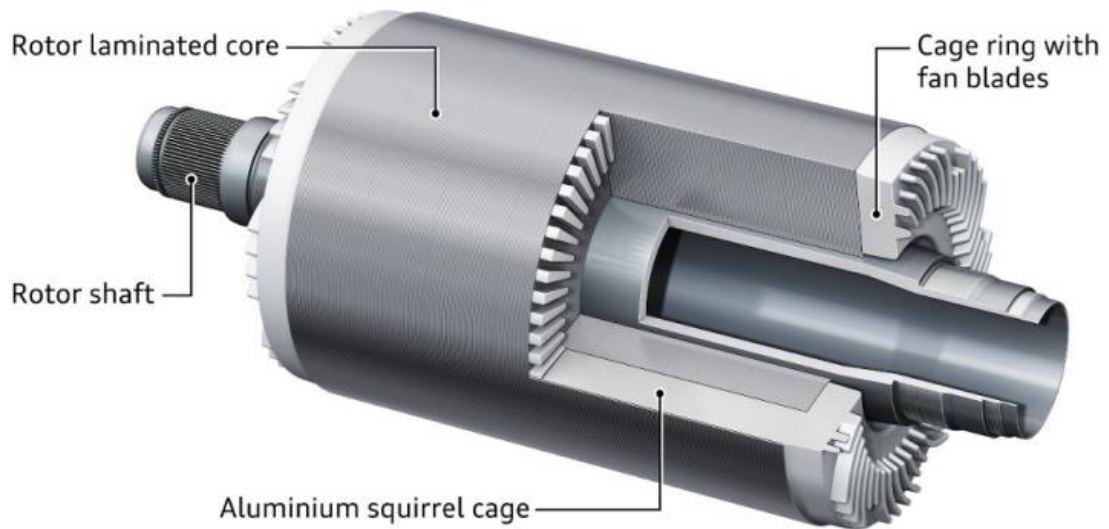
Figure 24. Audi e-tron induction rotor (Ardey et al. 2019, p. 16).

GE Motors Custom 8000 and Pegasus MHV induction motors have options for either copper or aluminum squirrel cage. Rotor laminations are punched from thin electrical grade steel sheet and coated with thermal insulation film. Squirrel cage bars on the outer surface are uninsulated. Power output of squirrel cage induction motors ranges from 100 to 20 000 hp. (GE Motors 2008, p. 2, 5.) Rotor constructions for GE Motors copper and aluminum rotors can be seen in Figure 25 below.
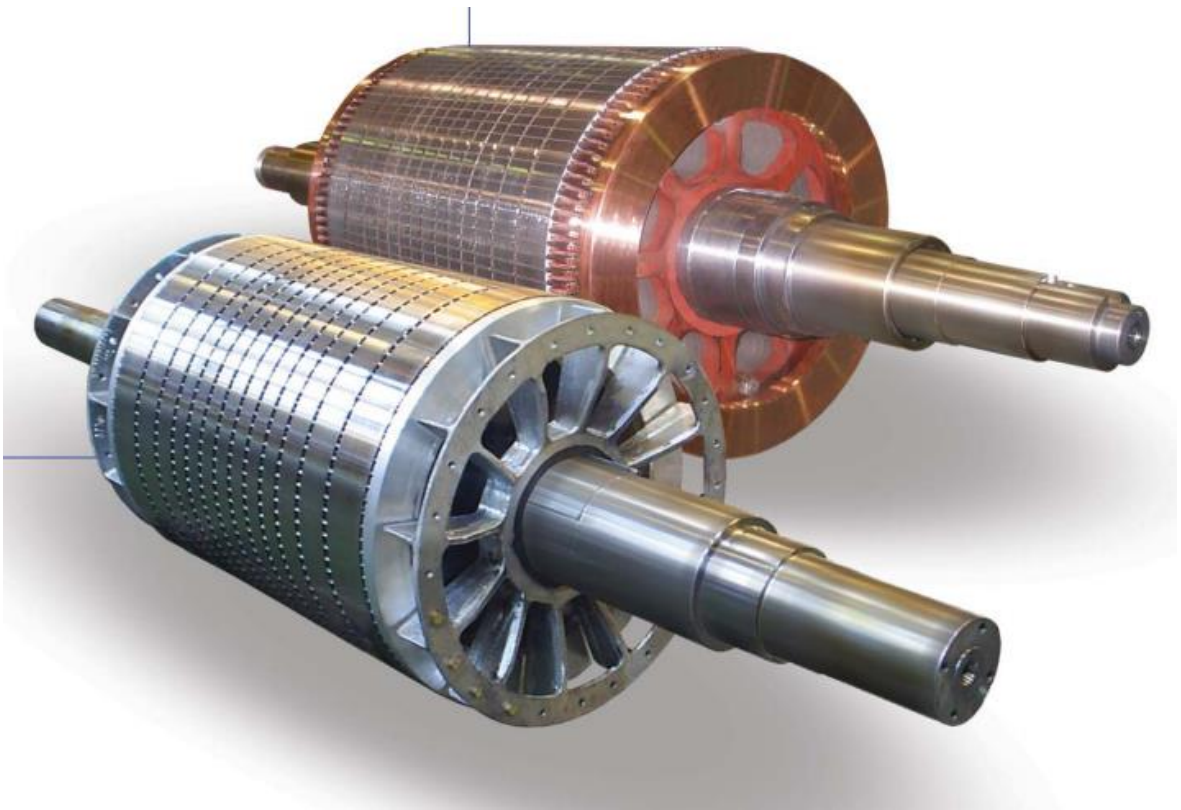
Figure 25. GE Motors aluminum and copper squirrel cage rotors (GE Motors 2008, p. 5).

ABB HXR is lineup of rib cooled induction motors with power output up to 2250 kW and synchronous speeds ranging from 500 to 3600 rpm (ABB 2021, p. 124.) HXR motors usually use deep bars of copper in the squirrel cage, but the bars can be made from copper alloy or aluminum alloy instead. Bars are brazed or welded to the end rings depending on the material. Vibration displacement at 3600 rpm is less than 0.3 mils. At 2 MW output, efficiency of the motor is at 97.7 %. (ABB 2009, p. 5-7.) Picture of the ABB HXR rotor can be seen in Figure 26 below.
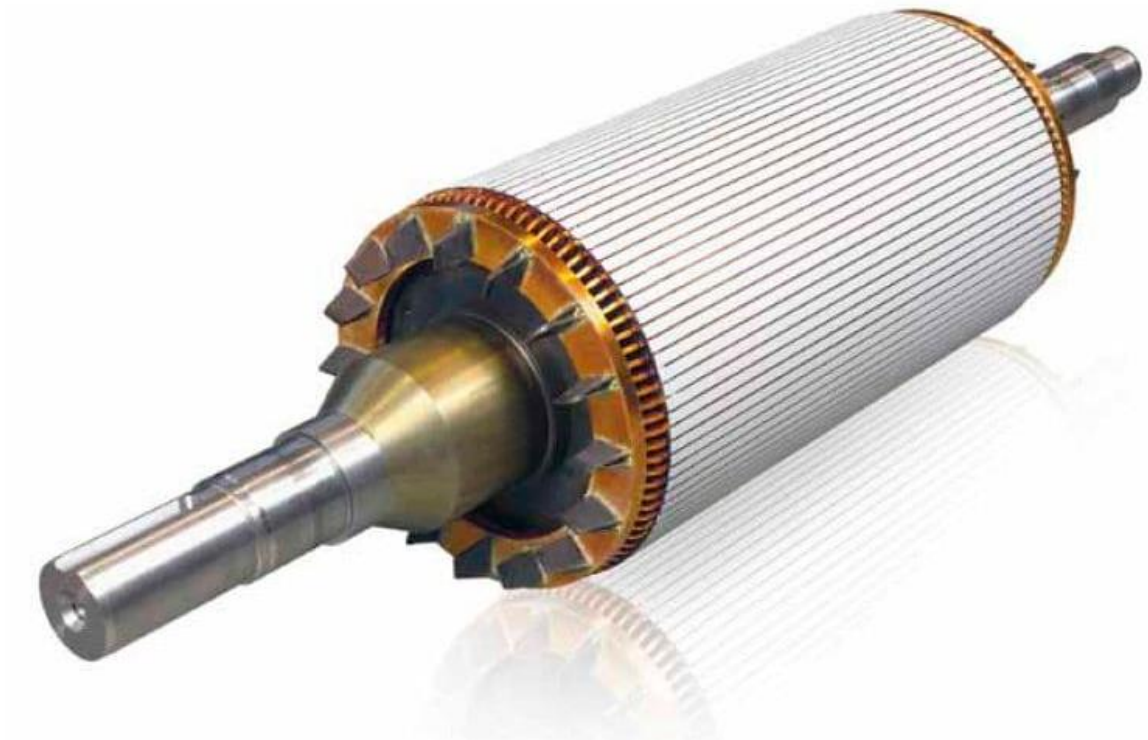
Figure 26. ABB HXR rib cooled induction machine rotor (ABB 2009, p. 7.)

Information regarding commercial induction machine rotor constructions and specifications tends to be quite scarce but from the limited review, some trends can be observed. Induction motors with high power output are limited to relatively low rpm and vice versa motors with high rpm have relatively low power output. Reasons for the limited low rpm could be caused by the materials and construction used in the rotor. Laminations used are thin electrical steel, which improves electrical properties to the detriment of mechanical strength. Another weakness could be the use of copper or aluminum instead of alloys which again sacrifices the mechanical strength for improved electrical conductivity. Common shape for the squirrel cage bars seems to be tall and narrow spear head shape towards the center of the rotor.

4.7   Discussion

This thesis strives to answer research questions from chapter 1.7 regarding on how to improve manufacturability or mechanical strength of the laminated induction rotor and fulfill aims and objectives from chapter 1.8 where manufacturing methods and materials are reviewed. Options are reviewed regarding the construction and materials which creates the framework to find the optimal solution. There are quite a lot of variables and ever-changing design that makes it difficult to finalize any solutions.

Limitations of the research stem from the number of unknowns and lack of data. Proposed solutions are more or less subjective estimations on what could work. Manufacturing processes are also difficult to estimate in terms of manufacturing time and cost due to variance in process parameters and lack of comparable up to date information between processes. Further research possibilities include comprehensive testing of processes and materials for accurate comparison from which decision could be made without too much guessing. Another research possibility could be testing of different coating options for the lamination disks. There are quite a lot of variables on the effectiveness, methods and price of the coating which could be reviewed further. Last research possibility could be building prototype of the proposed construction and analyzing the pros and cons from which changes can be made to improve the design.

5 PROPOSED CONSTRUCTION

Proposed construction is subjectively optimal final construction based on the analyzed solutions. Better alternatives for processes and materials may arise on further research and there can be changes in the design which affects the optimal construction.

Shaft made out from S355 can be manufactured from round bar cut to length by band saw. Machined features on the shaft include flat surfaces on the side, half a dozen shoulders, two threads and two ground surfaces for the active magnetic bearings. Every machining operation should be able to be done with large enough 4-axis mill-turn with grinding accessories.

Lamination disks made from S960 or softer material, if possible, have more options in terms of manufacturing. Fine blanking should be optimal for thin disks. Increasing the thickness until capabilities of fine blanking fall off at around 4-5 mm and punch laser combination machine becomes optimal process. Increasing thickness from that to over 8 mm and fiber laser is pretty much only viable solution. Cut off thickness between processes varies depending on the material and profile of the disk. Cut disks should be deburred and grinded for which there are multifunction grinding machines.

For the coating and insulation of the disks there are multiple options which could theoretically work. Desired properties for the coating include electrical resistivity and thermal conductivity which can be found in different coatings to varying degrees of effectivity. Polytetrafluoroethylene (PTFE) coating seems potentially viable option and depending on the effectiveness of the coating, every second disk being coated might be sufficient insulation between laminations. Depending on the design and requirements for the disk, other options could work just as well or better. After coating, contact surface for the shrink fit should be broached in order to get sufficient quality and tolerances for the assembly.

End disk made out of Inconel, or softer material, if possible, can be cut from plate with plasma cutting due to high thickness. End disk can be forged to shape and finished by

machining the threads, holes, and surfaces in 4-axis mill-turn. With softer material it may be viable to machine end disk from billet without forging.

End disk nut made from S355 can be cut from round bar with band saw and machined in multi-axis mill-turn. Machining includes milling of the flat surfaces on the outside, drilling, boring and threading of the hole in the inside.

Assembly of the rotor can be done with combination of cooling the shaft and heating the preassembled lamination stack on temporary shaft to get light shrink fit between the shaft and the lamination stack. On one end of the shaft, end disk and end disk nut and copper ring are pre-assembled to catch the lamination stack on installation. Cooling can be done with large enough constant temperature chamber up to -50 °C. Lamination stack with copper rods and spring pins is heated on temporary shaft and dropped vertically to the final shaft on install, guided by the flat surfaces on the shaft and lamination disks. The other end disk, copper ring and end disk nut are installed. Axial pressure is applied on the lamination stack from the end disks and end disk nut is tightened to keep the pressure on the stack. copper rod ends can be upset forged into the copper rings to short circuit the squirrel cage. Surface of the rotor is machined on lathe to optimize the rod distance to the surface of the rotor. After assembly and machining of the surface, rotor is balanced after which it should be ready for the further assembly of the induction machine.

6   CONCLUSION

Laminated squirrel cage induction machine rotor constructions all have similar structure but variables and options in terms of design and manufacturing are endless. Balance between electrical and mechanical properties should be optimized where mechanical strength is sufficient to withstand the rotational forces while electrical properties, such as squirrel cage conductivity and lamination disk insulation, should be improved. Some commercial squirrel cage rotors are examined briefly. Power output of 2 MW combined with 15 000 rpm requires sturdier structure compared to low rpm or low power induction machines. Design and construction of the rotor used is single design from the iterative loop of concurrent engineering and things are subject to change as project progresses. Laminated squirrel cage induction machine construction and working principle is examined briefly along with viable machining and coating processes. Rotor construction is divided into four main parts, excluding copper end ring and bars, and options are reviewed in terms of materials and processes to find optimal solutions for each part. Subjectively optimal proposed construction and assembly is formed from the viable options for each main part.

Options for manufacturing are reviewed and improvement in manufacturability depends on the starting point. Some of the reviewed options might provide some improvement over current manufacturing methods or processes but it all depends on the design and requirements whether one option would be better than the other. Improvement on mechanical strength of the rotor is more on the field of design and material selection than in the manufacturability of the components but if required, parts can be made out of higher strength material and options regarding manufacturability would adjust accordingly. This thesis focuses on single design with predefined dimensions and materials and provides subjectively optimal proposed construction for the manufacturability of the laminated squirrel cage induction rotor. More accurate results could be obtained with further research and testing to evaluate and compare different processes and materials.

LIST OF REFERENCES

Aarniovuori, L., Agamloh, E. B., Cao, W., Niemelä, M., Pyrhönen, J. 2018. Loss Components and Performance of Modern Induction Motors. 2018 XIII International Conference on Electrical Machines (ICEM). pp. 1253-1259.

ABB. 2009. High voltage cast iron motors Up to 2250 kW, 3000 HP. [web document]. [referred 19.8.2021]. Available: https://pdf.nauticexpo.com/pdf/abb-marine/pdf-brochure-high-voltage-cast-iron-motors-hxr/30709-96010.html.

ABB. 2021. High voltage engineered induction motors Technical catalog. [web document]. [referred 19.8.2021]. Available: https://search.abb.com/library/Download.aspx?DocumentID=9AKK103508&LanguageCode=en&DocumentPartId=&Action=Launch.

Agamloh, E., Kaufman Dyes, N. 2007. Copper Rotor Motors: A Step toward Economical Super-Premium Efficiency Motors? ACEEE Summer Study on Energy Efficiency in Industry. pp. 65-74.

American Beryllia Inc. n.d. Beryllium Oxide. [American Beryllia Inc. webpage]. [referred 15.7.2021]. Available: https://www.americanberyllia.com/beryllium-oxide.

Annaka, S., Fujii, S., Hirakuri, K., Kuwabara, H., Nakajima, D., Tanaka, Y. 2020. Diamond-like carbon coating for effective electrical insulation of Cu and Al wires. Diamond and Related Materials, 103: 107731. 6 p.

AOTCO. 2015. Metal Finishing with Beryllium Oxide. [AOTCO webpage]. [referred 15.7.2021]. Available: https://www.aotco.com/blog/metal-finishing-with-beryllium-oxide.

Ardey, N., Doerr, J., Fröhlich, G., Laudenbach, T., Mendl, G., Straßer, R. 2019. The new full electric drivetrain of the Audi e-tron. Liebl J. (eds) Der Antrieb von morgen 2019. Springer Vieweg, Wiesbaden. 25 p.

Azarmi, F., Mironov, E., Safonov, A., Shakhova, I. 2017. Thermo-electrical properties of the alumina coatings deposited by different thermal spraying technologies. Ceramics International 43 (2017). Elsevier Ltd and Techna Group S.r.l. pp. 15392-15401.

Barta, J., Uzhegov, N., Losak, P., Ondrusek, C., Mach, M. & Pyrhönen, J. 2019. Squirrel Cage Rotor Design and Manufacturing for High-Speed Applications. IEEE Transactions on Industrial Electronics, 66: 9. pp. 6768-6778.

Bhattacharyya, B. & Doloi, B. 2020. Modern Machining Technology: Advanced, Hybrid, Micro Machining and Super Finishing Technology. Academic Press. 763 p.

Boglietti, A., Brown, N. L., Cavagnino, A., Gerada, C., Gerada, D. & Mebarki, A. 2014. High-Speed Electrical Machines: Technologies, Trends, and Developments. IEEE Transactions on Industrial Electronics, 61: 6. pp. 2946-2959.

Booker, J. D., Swift, K. G. 2013. Manufacturing Process Selection Handbook. Butterworth-Heinemann. 433 p.

Boulter, E. A., Culbert, I., Dhirani, H., Stone, G. C. 2014. Electrical insulation for rotating machines: design, evaluation, aging, testing, and repair. Second edition. Wiley. 643 p.

Cavallo, C. n.d. What is a Squirrel Cage Motor and How Does it Work? [web document]. [referred 13.9.2021]. Available: https://www.thomasnet.com/articles/machinery-tools-supplies/what-is-a-squirrel-cage-motor-and-how-does-it-work/.

Chazal, H., Garbuio, L., Gerbaud, L., Thomas, R. 2020. Modeling and design analysis of the Tesla Model S induction motor. 2020 International Conference on Electrical Machines (ICEM). 7 p.

Cope, M. n.d. AN INTRODUCTION TO MILL-TURN TECHNOLOGY. [web document]. [referred 27.5.2021]. Available: https://blog.hurco.com/blog/bid/281989/an-introduction-to-mill-turn-technology.

Copper Development Association. n.d. [Copper Development Association webpage]. [referred 27.5.2021]. Available: https://copperalliance.org.uk/about-copper/conductivity-materials/copper-zirconium/.

Davim, J. P., Kalita, H., Kumar, K., Zindani, D. 2019. Materials and Manufacturing Processes. Materials Forming, Machining and Tribology. Springer International Publishing. 104 p.

Dhanumalayan, E., Joshi, G. M. 2018. Performance properties and applications of polytetrafluoroethylene (PTFE) — a review. Advanced Composites and Hybrid Materials (2018). pp. 247-268.

Durantay, L., Fontini, J., Mauffrey, T., Pradurat, J-F. 2013. Comparison of 5 different squirrel cage rotor designs for large high speed induction motors. PCIC Europe 2013. 9 p.

EMERSON 2017. PTFE and PFA Similarities and Differences. [web document]. [referred 2.9.2021]. Available: https://www.emerson.com/documents/automation/white-paper-ptfe-pfa-similarities-differences-rosemount-en-585104.pdf.

Evans, K. 2016. Programming of CNC Machines. 4th edition. Industrial Press. 500 p.

GE Motors. 2008. Induction & Synchronous Motors. [web document]. [referred 5.8.2021]. Available: https://nemsco.com/wp-content/uploads/2017/04/ge-induction-synchronous.pdf.

Groover, M. P. 2010. Fundamentals of Modern Manufacturing: Materials, Processes, and Systems. 4th edition. Wiley. 1012 p.

Groover, M. P. 2019. Fundamentals of Modern Manufacturing: Materials, Processes, and Systems. 7th edition. Wiley. 816 p.

Imai, Y., Kakuta, N., Mabuchi, K., Okuyama, N., Yamada, Y., Watanabe, M. 2004. Diamond-like Carbon Coating on Micropipettes. The 26th Annual International Conference of the IEEE Engineering in Medicine and Biology Society. pp. 2454-2457.

iPolymer 2018. Comparisons: Which Type of Fluoropolymer Coating Should You Use? [iPolymer webpage]. [referred 2.9.2021]. Available: https://www.ipolymer.com/blog/fluoropolymer-coating-which-should-you-use/.

Kliman, G. B. (editor), Toliyat, H. A. (editor) 2004. Handbook of electric motors. Second edition. CRC Press. 778 p.

LENOX n.d. Guide to band sawing. [web document]. [referred 11.9.2021]. Available: https://www.lenoxtools.com/Guides/LENOX_20Guide_20to_20Band_20Sawing.pdf.

Luminoso, L. 2019. The added benefits of punch/laser combination machines. [web document]. [referred 10.6.2021]. Available: https://www.canadianmetalworking.com/canadianfabricatingandwelding/article/fabricating/the-added-benefits-of-punch-laser-combination-machines.

Manney, D. 2017. What Role do Laminations Play in Electric Motors and Generators? [web document]. [referred 13.9.2021]. Available: https://manney.medium.com/what-role-do-laminations-play-in-electric-motors-and-generators-20ce894f6a78.

Matrix Coatings. n.d. [Matrix Coatings webpage]. [referred 19.8.2021]. Available: https://matrixcoat.com/teflon-coatings-resources/.

Melkebeek, J. A. 2018. Electrical Machines and Drives: Fundamentals and Advanced Modelling. Springer International Publishing AG. 731 p.

Mullen, C. 2018. How to Estimate CNC Machining Time. [web document]. [referred 17.6.2021]. Available: https://careertrend.com/how-5838260-estimate-cnc-machining-time.html

Naiju, C. D. 2021. DFMA for product designers: A review. Materials Today: Proceedings. 6 p.

Palupi, A. E., Riandadari, D., Sakti, A. M. 2020. The Effect of Heating Time and Heating Temperature to Layer Thickness and The Glossiness Level of A Surface in Blackening Coating Process. International Journal of Innovative Technology and Exploring Engineering (IJITEE), 9: 3S. pp. 250-254.

Pat. US 8,154,167 B2. 2012. INDUCTION MOTOR LAMINATION DESIGN. Tesla Motors, Inc. (Yifan, T.) Appl. 13/074,841, 2011-03-23. Publ. 2012-04-10. 26 p.

SFS-EN 10029. Hot-rolled steel plates 3mm thick or above. Tolerances on dimensions and shape. Helsinki: Suomen Standardisoimiliitto SFS, 2011. 12 p. Confirmed 24.1.2011.

Special Metals. n.d. PRODUCT HANDBOOK OF HIGH-PERFORMANCE NICKEL ALLOYS. [web document]. [referred 27.5.2021]. Available: https://www.specialmetals.com/documents/nickel-alloy-handbook.pdf.

SSAB. n.d.a [SSAB webpage]. [Referred 27.5.2021]. Available: https://www.ssab.com/products/brands/strenx/products/strenx-960-mc.

SSAB. n.d.b. Hardox guarantees. [web document]. [referred 2.9.2021]. Available: https://www.ssab.fi/tuotteet/brandit/hardox/hardox-download.

Velling, A. 2019. Structural Steels S235, S275, S355, S420 and Their Properties. [web document]. Published 7.1.2019. [referred 27.5.2021]. Available: https://fractory.com/structural-steels-s235-s275-s355-s420-and-their-properties/.

Wilson Tool. 2013. A Closer Look at Punching Force. [Wilson Tool webpage]. [referred 19.9.2021]. Available: https://www.wilsontool.com/WilsonTool/files/31/31089b11-052b-451c-bb05-cd56aee1b9d2.pdf.